Exploring the Long Wavelength Universe with Radio Telescopes

Anna Scaife

CAPPA School on High Energy Astrophysics,

Dublin 8th July

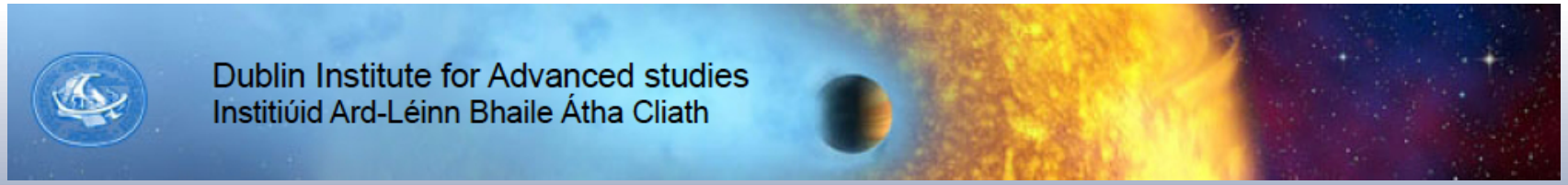

Outline

1. **The Radio Waveband**
2. **Single Dish Radio Telescopes**
3. **High Radio Frequency Science**
   - Thermal Bremsstrahlung
   - The Sunyaev–Zel'dovich (SZ) Effect
4. **Radio Interferometry**
5. **Low Frequency Science**
   - Low Frequency Synchrotron Emission
6. **Reading List**

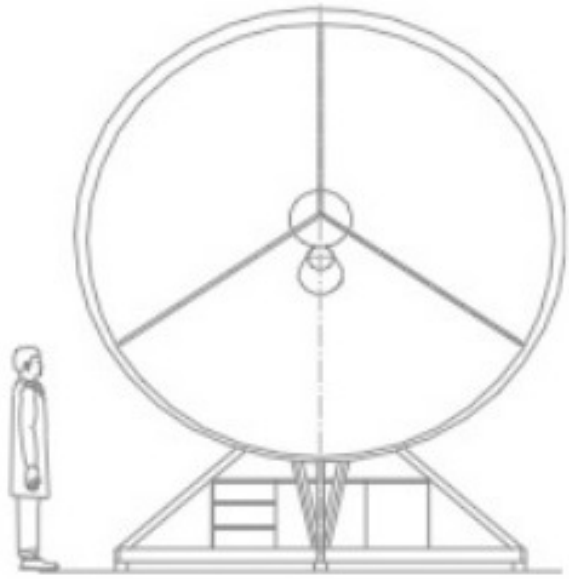

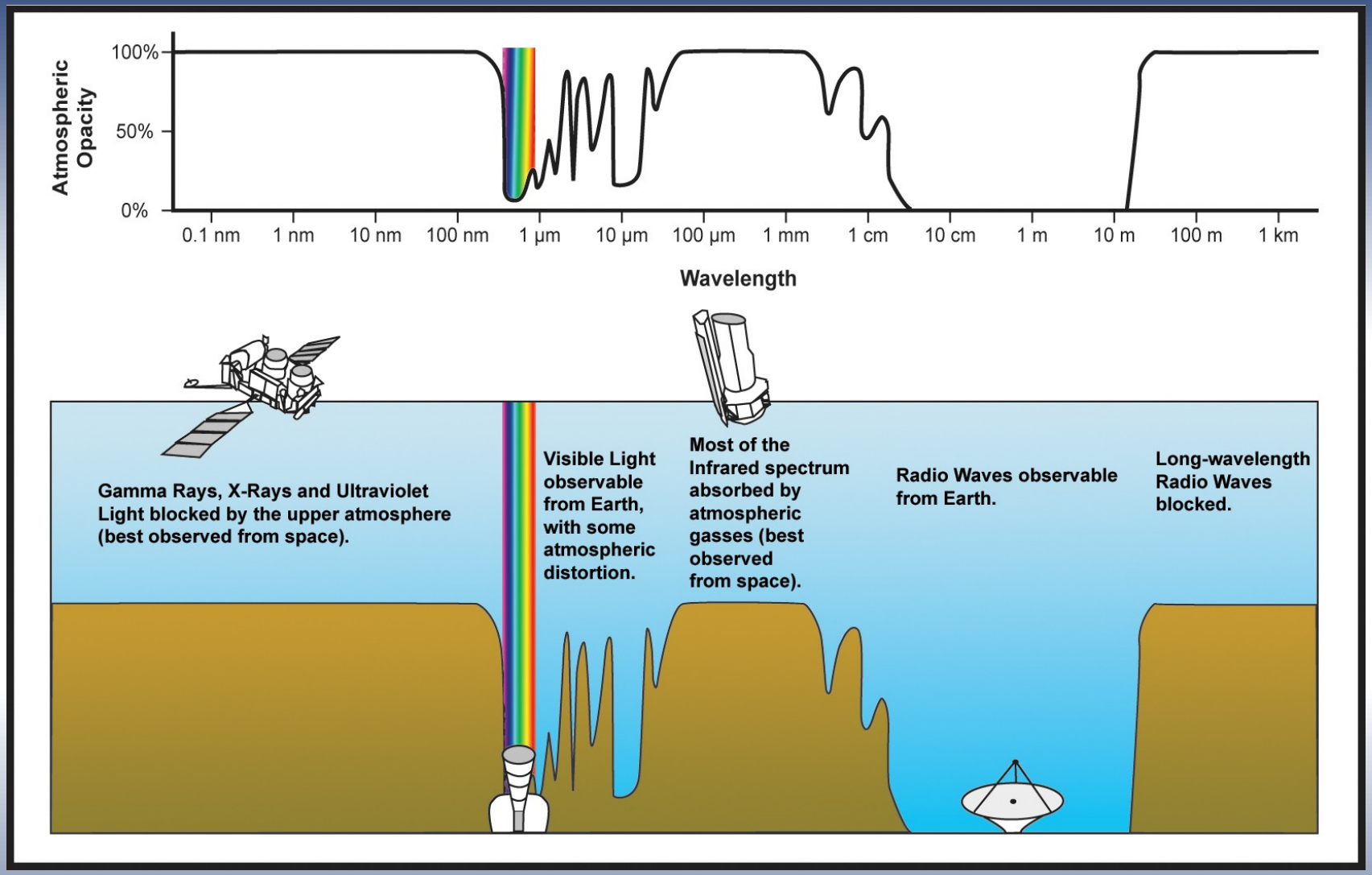
Atmospheric Opacity
100%
50%
0%
0.1 nm
1 nm
10 nm
100 nm
1 μm
10 μm
100 μm
1 mm
1 cm
10 cm
1 m
10 m
100 m
1 km
Wavelength
Gamma Rays, X-Rays and Ultraviolet Light blocked by the upper atmosphere (best observed from space).
Visible Light observable from Earth, with some atmospheric distortion.
Most of the Infrared spectrum absorbed by atmospheric gasses (best observed from space).
Radio Waves observable from Earth.
Long-wavelength Radio Waves blocked.

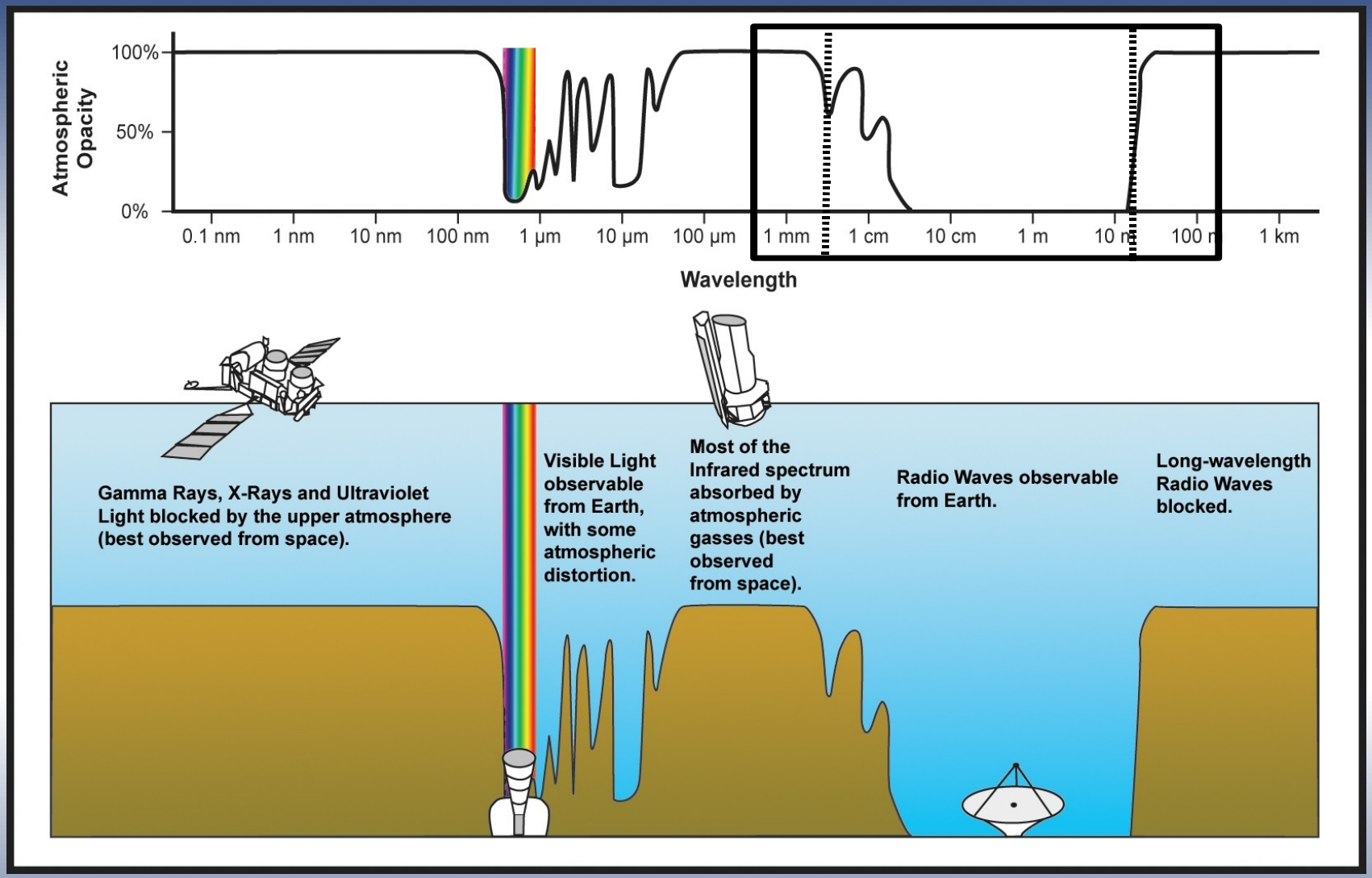
Atmospheric Opacity
100%
50%
0%
0.1 nm
1 nm
10 nm
100 nm
1 μm
10 μm
100 μm
1 mm
1 cm
10 cm
1 m
10 m
100 m
1 km
Wavelength
Gamma Rays, X-Rays and Ultraviolet Light blocked by the upper atmosphere (best observed from space).
Visible Light observable from Earth, with some atmospheric distortion.
Most of the Infrared spectrum absorbed by atmospheric gasses (best observed from space).
Radio Waves observable from Earth.
Long-wavelength Radio Waves blocked.

Early Radio Astronomy

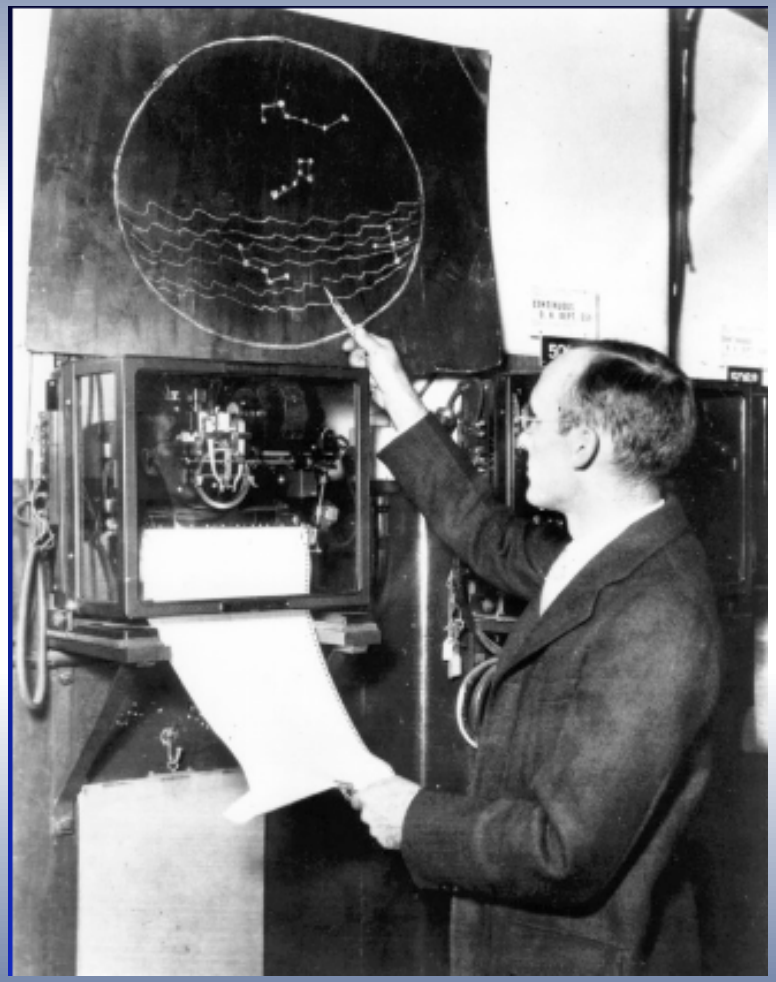

(credit: NRAO/AU)

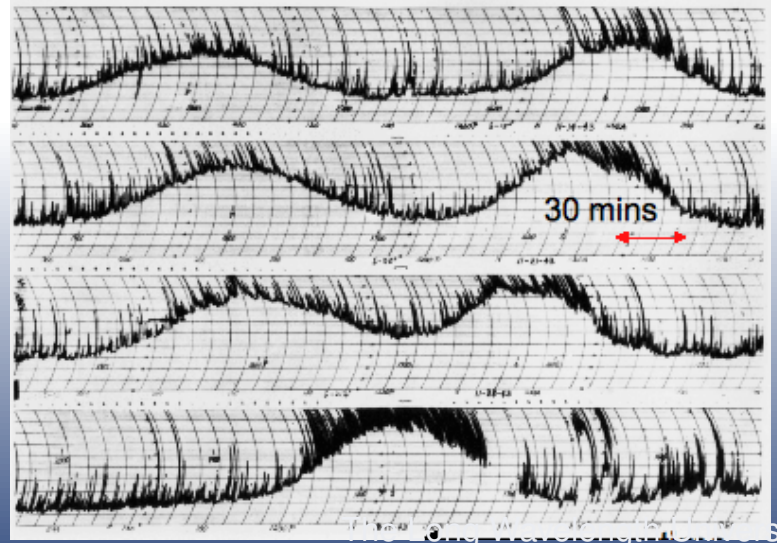

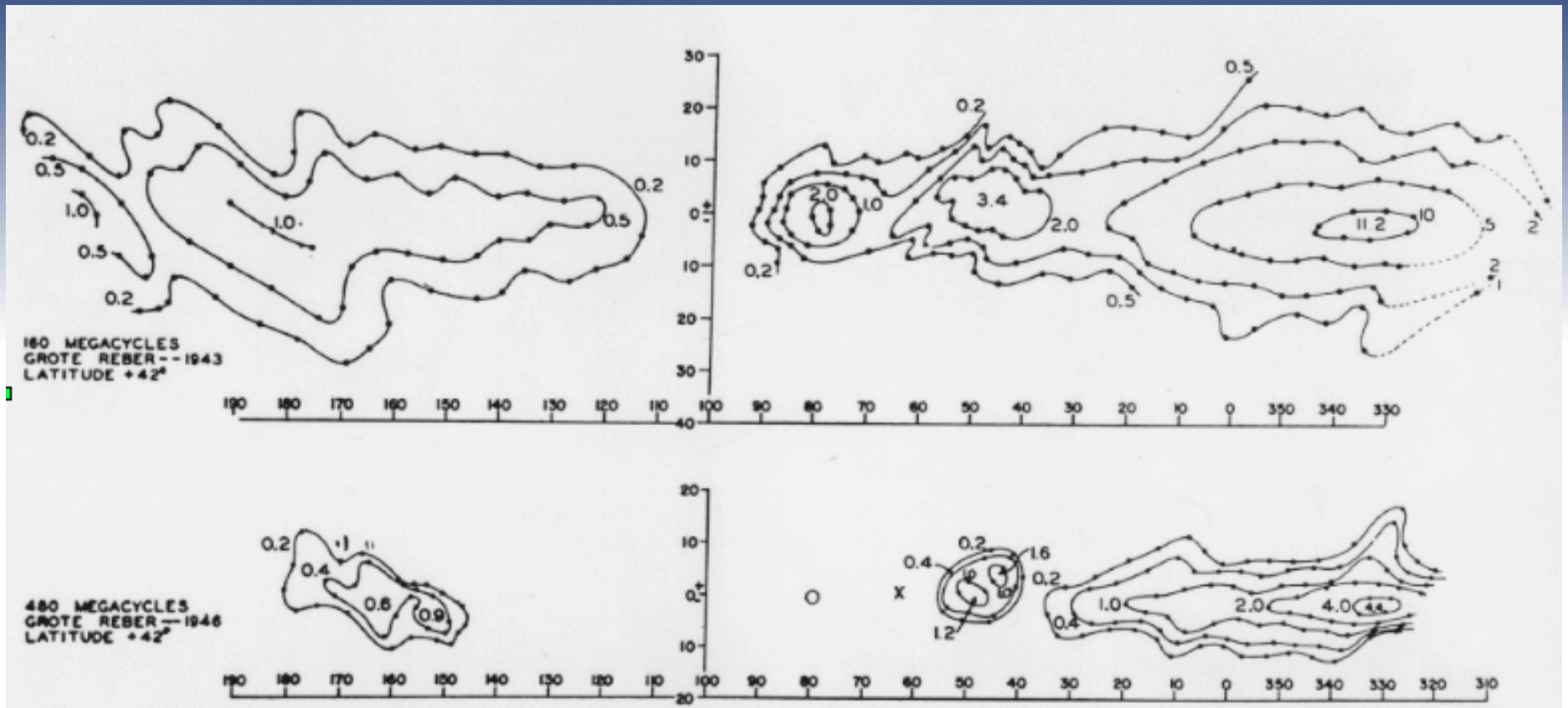

FIG. 7—Contours of constant intensity at 160 MHz and 480 MHz, taken at Wheaton, Illinois.

"Galactic Radio Waves", G. Reber, Sky and Telescope, Vol. 8, No. 6, April 1949

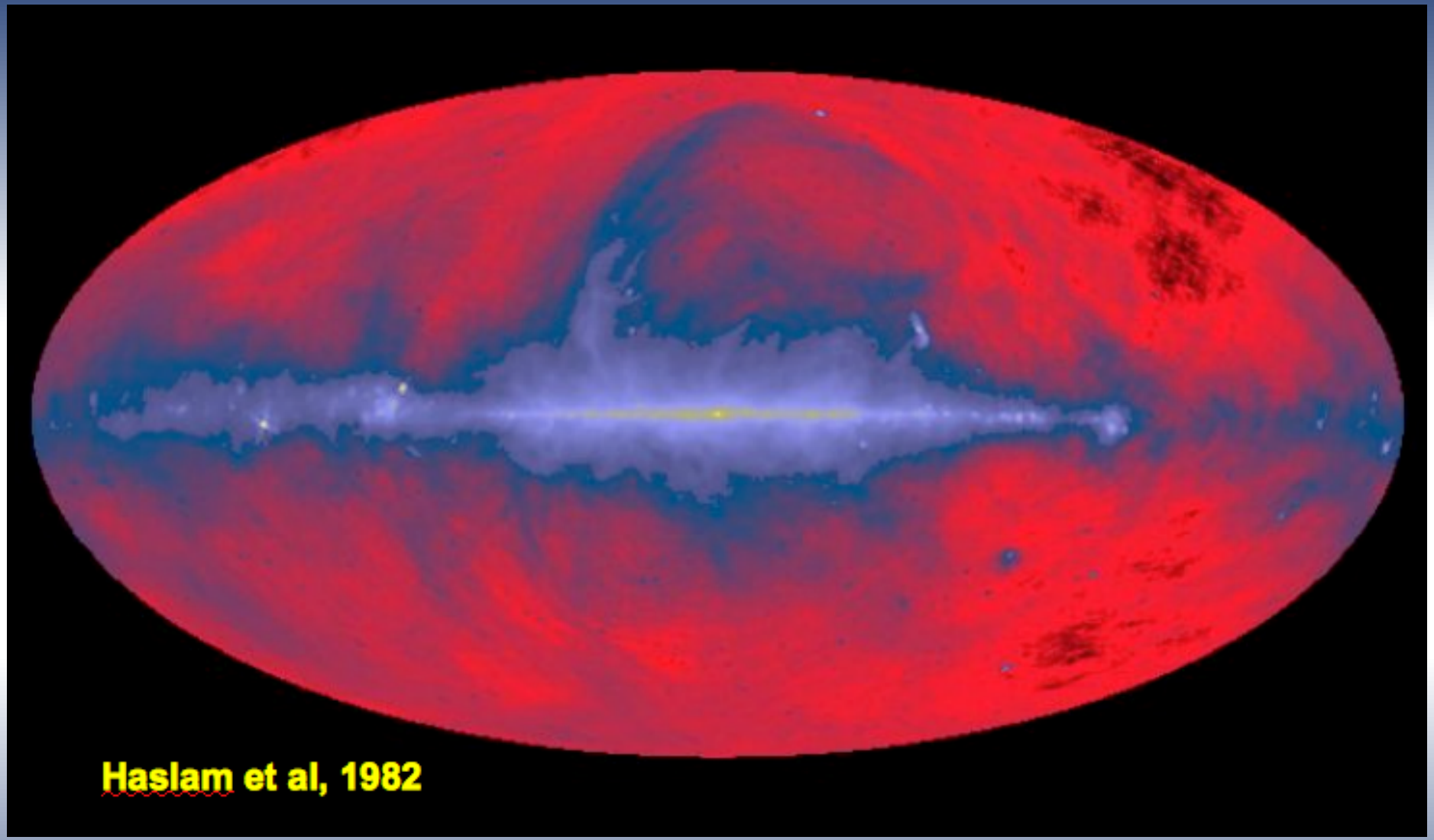
Haslam et al, 1982

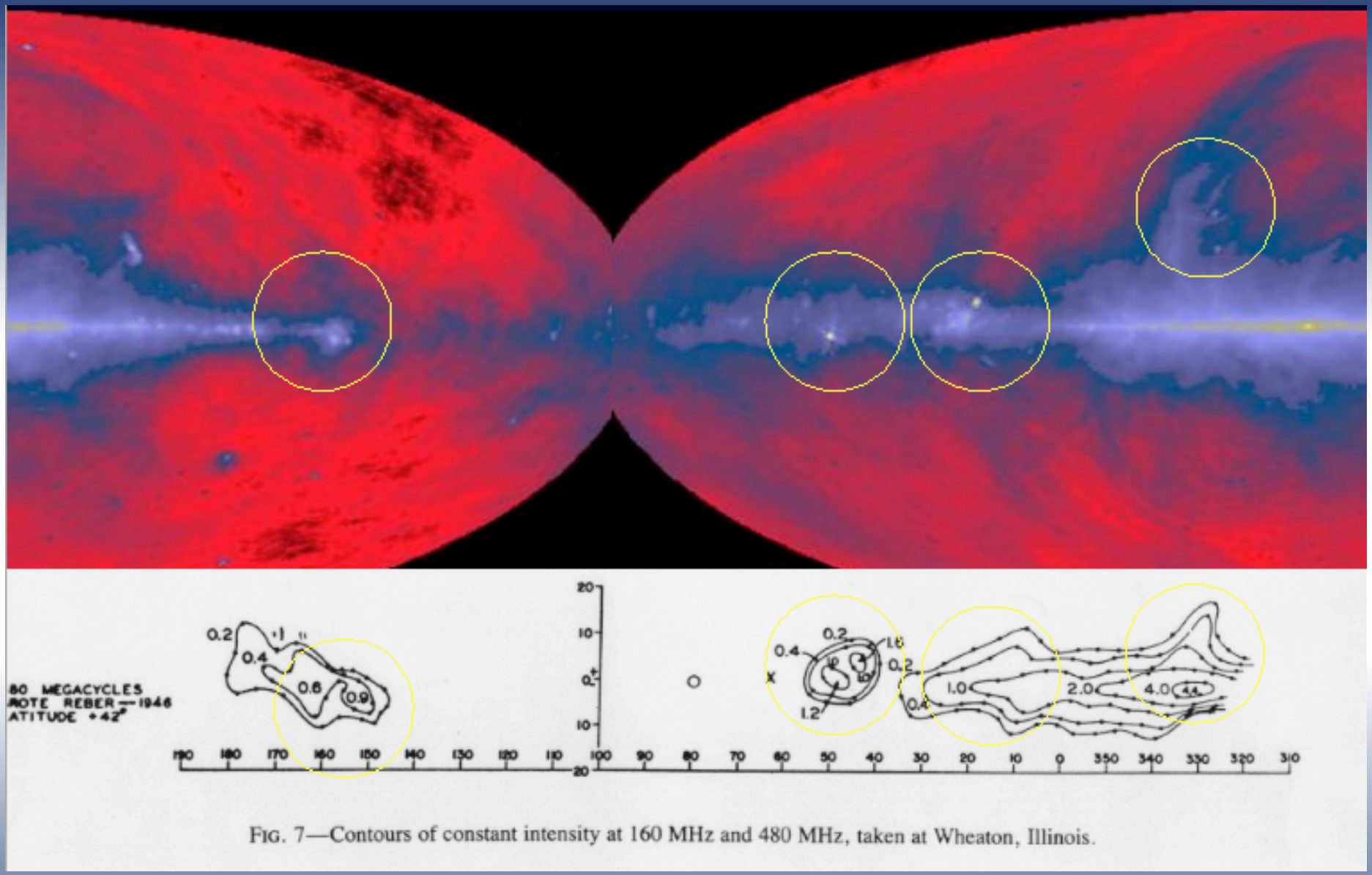

FIG. 7—Contours of constant intensity at 160 MHz and 480 MHz, taken at Wheaton, Illinois.

Cut-off Points

The radio waveband extends from 30 m (10 MHz) to 3 mm (100 GHz)

At either end of this waveband the atmosphere causes a cut-off

At the high frequency end the troposphere is the problem

At the low frequency end the ionosphere is the problem

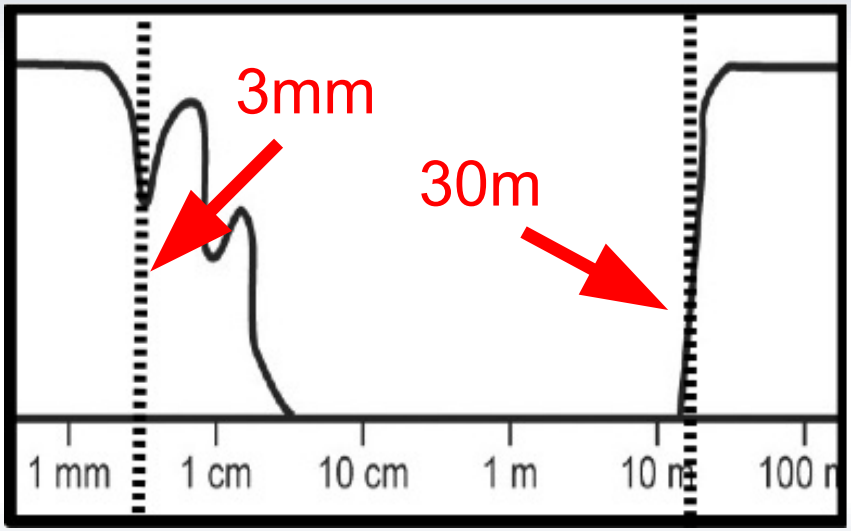

Cut-off Points

The radio waveband extends from 30 m (10 MHz) to 3 mm (100 GHz)

At either end of this waveband the atmosphere causes a cut-off

At the high frequency end the troposphere is the problem

At the low frequency end the ionosphere is the problem

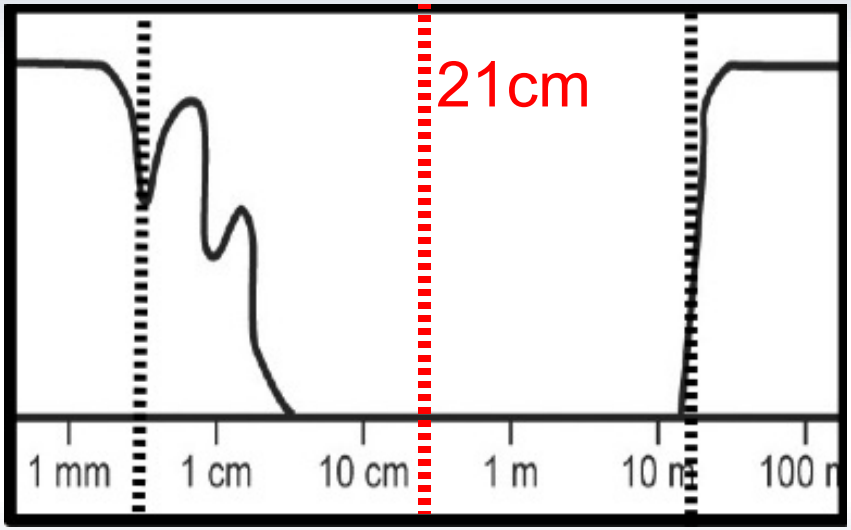

Cut-off Points

The radio waveband covers 3 orders of magnitude in wavelength

Such a range of wavelengths require different types of telescope

In L1 we will cover the high frequency end of the band from 3 mm down to 21 cm

In L2 we will cover the low frequency end of the band from 21 cm down to 30 m

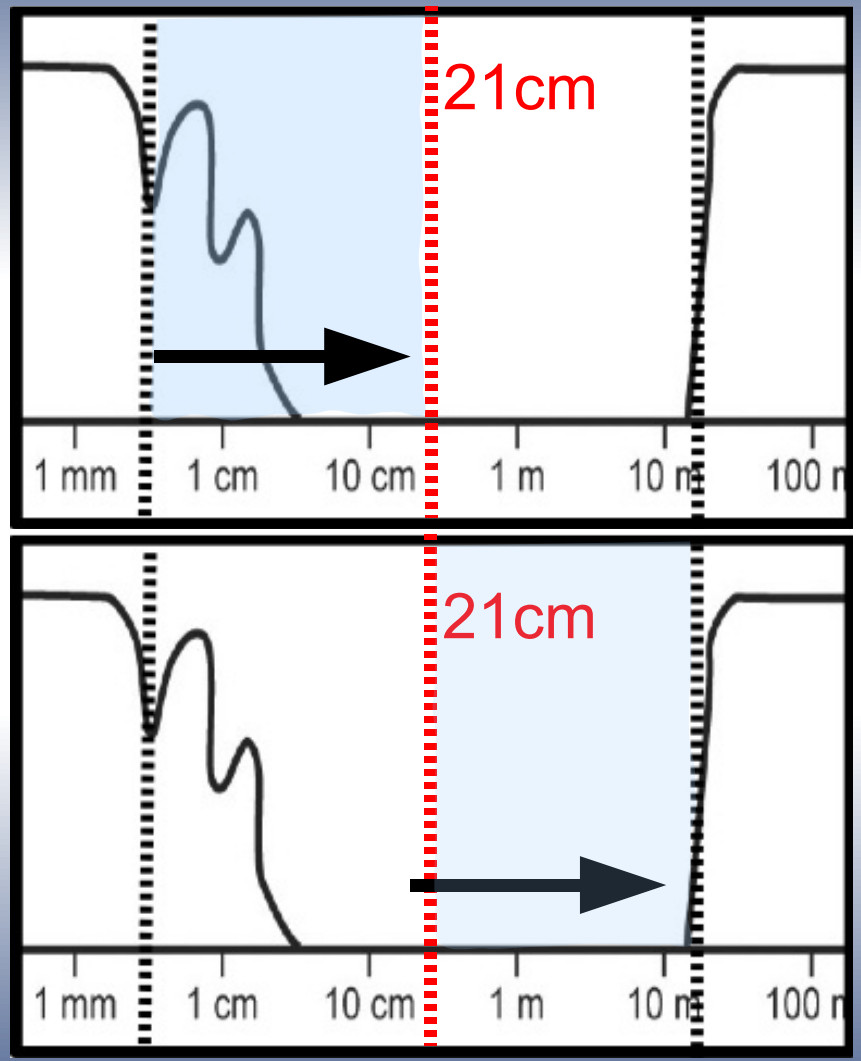

Major Emission Mechanisms

Thermal (vibrational) dust emission dominates at high frequencies: $S_\nu \propto \nu^4$

Bremsstrahlung (free-free) emission dominates at intermediate frequencies: $S_\nu \propto \nu^{-0.1}$

Synchrotron emission dominates at low frequencies: $S_\nu \propto \nu^{-0.7}$

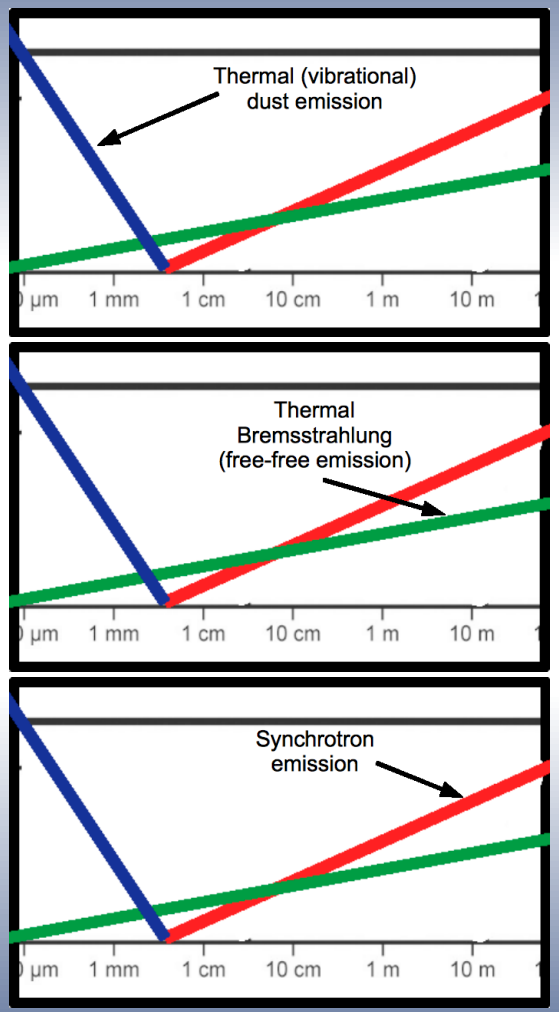

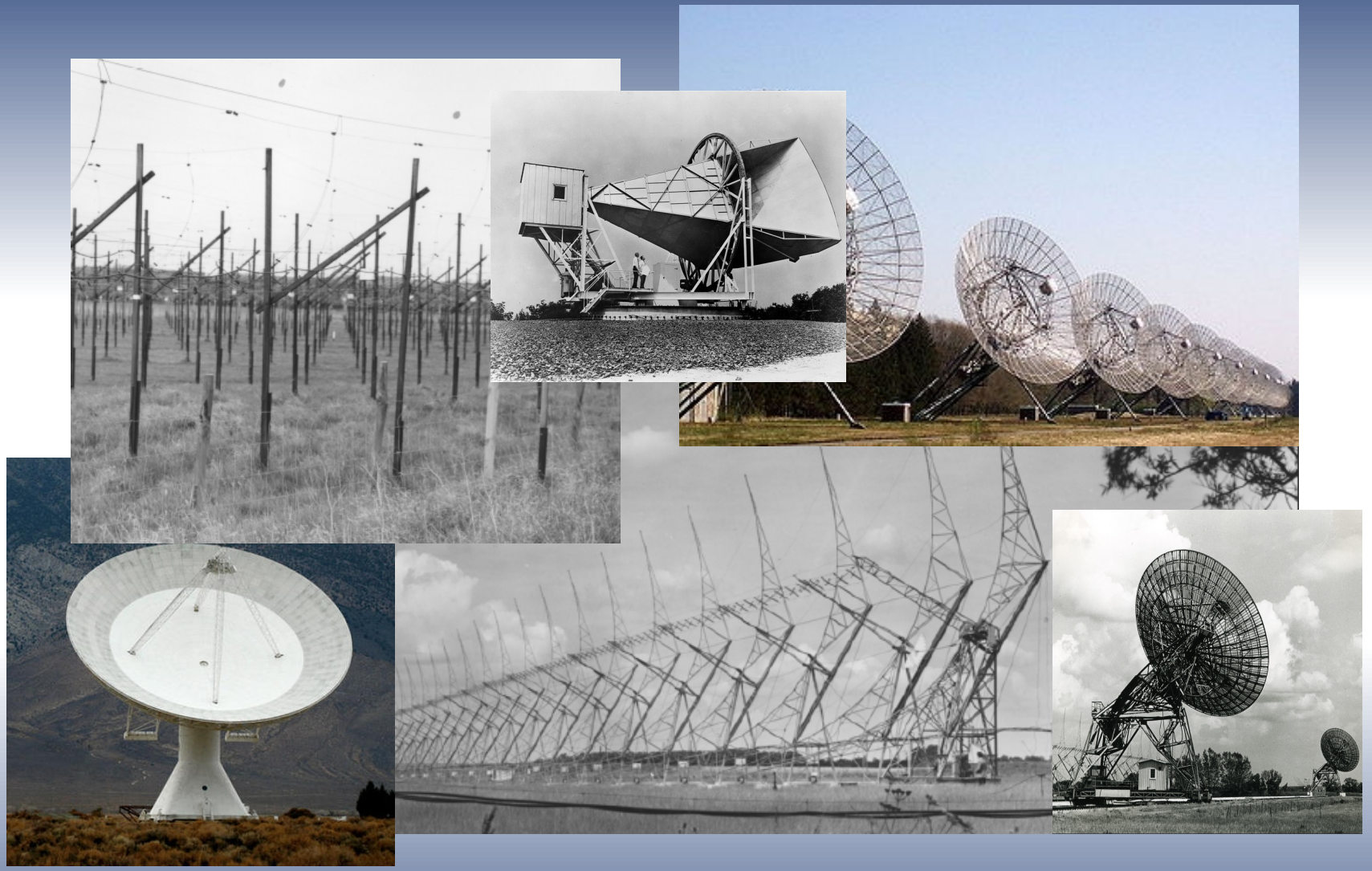

Single Dish Radio Telescopes

Some Basics

- Single dish telescopes are like single pixel cameras
- They need to be scanned across fields of view (FOV) to produce maps
- This can lead to poor systematics in the images
- They recover **total power** data

A typical single dish measurement will employ a beam switching strategy to implement a differencing scheme. This beam switching will usually be done by tilting a sub-reflector within the main dish so that the source under observation is observed in an interleaved fashion with an comparitively empty region of sky. This type of on–off observing is done in order to eliminate time-varying sky and instrumental effects.

Sensitivity

The sensitivity is related to the surface area:

$$\Delta S = \frac{2 k_{\mathrm{B}} T_{\mathrm{sys}}}{A_{\mathrm{eff}} \sqrt{B\tau}}$$

The effective area, A_{eff} , will be some fractional multiple of the true dish area, usually between 0.6 and 0.7, and arises as a consequence of the imperfect conduction on the dish surface.

Sensitivity

The sensitivity is related to the surface area:

$$\Delta S = \frac{2k_B T_{sys}}{A_{eff}\sqrt{B\ \tau}}$$

This noise can be reduced by:

1. increasing the bandwidth, B , of the signal being passed through the system
2. increasing the integration time, τ , of the signal.

The first of these measures reduces the correlation in the signal, which scales as $1/B$, and consequently increases the number of independent measurements. The second measure again increases the number of independent measurements by a factor τ, and so the relative uncertainty in a measurement of antenna temperature is also inversely proportional to the square root of the integration time. The antenna temperature has contributions not only from the source, but also from the receiver itself, the atmosphere and also contributions from any sidelobe structure in the beam.

Sensitivity

The sensitivity is related to the surface area:

$$\Delta S = \frac{2 k_B T_{sys}}{A_{eff} \sqrt{B \ \tau}}$$

This noise can be reduced by:

1. increasing the bandwidth, B, of the signal being passed through the system
2. increasing the integration time, τ, of the signal.

The first of these measures reduces the correlation in the signal, which scales as $1/B$, and consequently increases the number of independent measurements. The second measure again increases the number of independent measurements by a factor τ, and so the relative uncertainty in a measurement of antenna temperature is also inversely proportional to the square root of the integration time. The antenna temperature has contributions not only from the source, but also from the receiver itself, the atmosphere and also contributions from any sidelobe structure in the beam.

Sensitivity

The sensitivity is related to the surface area:

$$\Delta S = \frac{2k_B T_{sys}}{A_{eff}\sqrt{B\,\tau}}$$

This noise can be reduced by:

1. increasing the bandwidth, B, of the signal being passed through the system
2. increasing the integration time, τ, of the signal.

The first of these measures reduces the correlation in the signal, which scales as $1/B$, and consequently increases the number of independent measurements. The second measure again increases the number of independent measurements by a factor τ, and so the relative uncertainty in a measurement of antenna temperature is also inversely proportional to the square root of the integration time. The antenna temperature has contributions not only from the source, but also from the receiver itself, the atmosphere and also contributions from any sidelobe structure in the beam.

Resolution

It is often easier to calculate the gain of a transmitting antenna than the collecting area of a large radio telescope, just as it's easier in practice to measure the transmission pattern than to measure the reception power pattern of an antenna. This **reciprocity** between reception and transmission is used to simplify antenna calculations and measurements. **Reciprocity** can be understood via Maxwell's equations or by thermodynamic arguments.

An antenna can be treated either as a receiving device, gathering the incoming radiation field and conducting electrical signals to the output terminals, or as a transmitting system, launching electromagnetic waves outward. These two cases are equivalent because of time reversibility: the solutions of Maxwell's equations are valid when time is reversed. (Burke & Smith 1997)

The strong reciprocity theorem: If a voltage is applied to the terminals of an antenna A and the current is measured at the terminals of another antenna B, then an equal current (in both amplitude and phase) will appear at the terminals of A if the same voltage is applied to B

can be formally derived from Maxwell's equations (Rohlfs & Wilson).

The power pattern of an antenna is the same for transmitting and receiving

Resolution

The beam of a telescope is the Fourier Transform of the distribution of excitation currents on the surface of the receptor:

$$\tilde{F}(\mathbf{k}) = \int_{-\infty}^{\infty} f(\mathbf{x}) e^{-2\pi i \mathbf{k}\cdot\mathbf{x}} dx$$

$$\begin{aligned} j &\propto g(x)e^{i\omega t} \quad \text{(reciprocity)} \\ df &\propto g(x)\frac{e^{-2i\pi r/\lambda}}{r}dx \quad \text{(Huygens)} \\ r &\sim R + x\sin\theta = R + xl \quad \text{(Fraunhofer)} \\ df &\propto g(x)e^{-i2\pi R/\lambda}e^{-i2\pi xl/\lambda}dx \\ f(l) &= \int g(u)e^{-i2\pi ul}du \quad u = x/l \\ P &\propto f^2 \end{aligned}$$

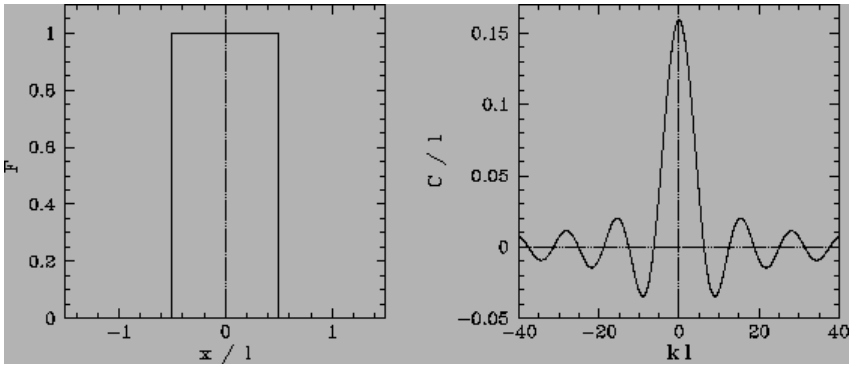

$$N(0,\sigma_x) \Leftrightarrow \tilde{N}(0,\sigma_k) \quad \sigma_k = 1/\sigma_x$$

The resolution is therefore inversely proportional to surface area:

$$\Delta\theta[\text{rad}] \approx \frac{\lambda}{D[\text{m}]}$$

100 m dish at λ =3 mm (100 GHz) $\Delta\theta \approx 6$ arcsec
100 m dish at λ =30 m (10 MHz) $\Delta\theta \approx 17$ degrees

Resolution

The data received is the sky signal **convolved** with the telescope beam:

$$f(x) * g(x) = \tilde{F}(k) \times \tilde{G}(k)$$

$$I'(l,m) = I(l,m) * A(l,m)$$

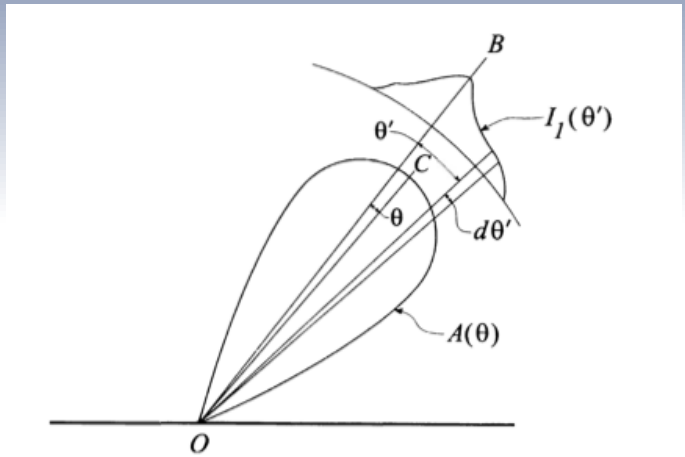

Consequently we recover maps in units of **Flux density per beam: Specific Intensity**

$$1 \text{ Jansky} = 10^{-26} \text{ Watts m}^{-2} \text{ Hz}^{-1}$$

Specific Intensity is related to brightness temperature:

$$I_\lambda(\text{Jy/beam}) = \frac{2k_B T_b}{\lambda^2}$$

Flux Density is related to brightness temperature:

$$S_\lambda(\text{Jy}) = \frac{2k_B T_b}{\lambda^2}\Omega$$

Cygnus X

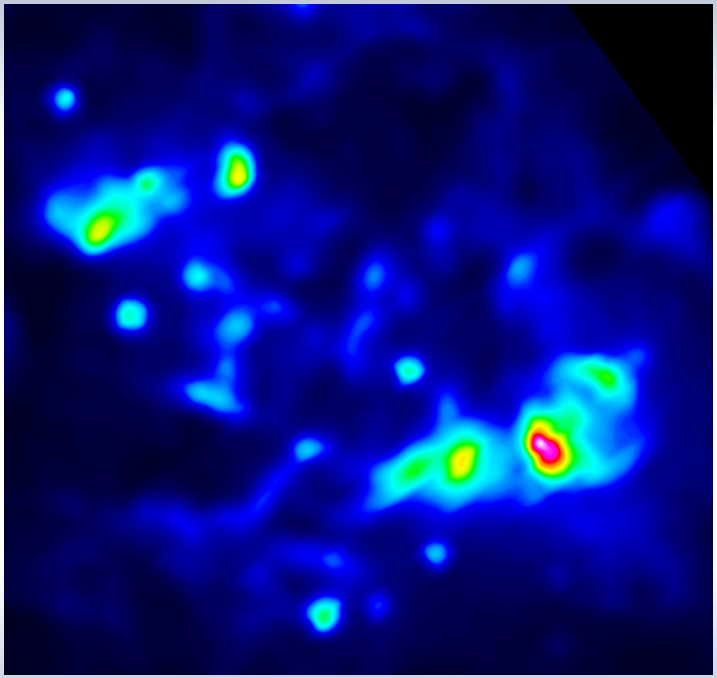

$\Delta\theta = 9$ arcmin

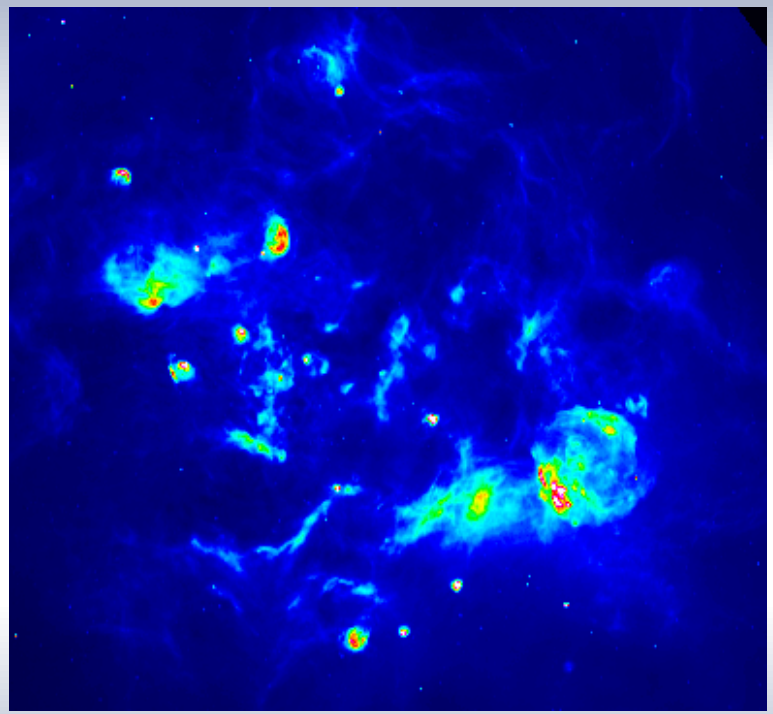

$\Delta\theta = 1$ arcmin

Outline

1. The Radio Waveband
2. Single Dish Radio Telescopes
3. **High Radio Frequency Science**
   - Thermal Bremsstrahlung
   - The Sunyaev–Zel'dovich (SZ) Effect
4. Radio Interferometry
5. Low Frequency Science
   - Low Frequency Synchrotron Emission
6. Reading List

Bremsstrahlung Emission

Emission due to the acceleration of an electron in the electrostatic field of a high energy proton or nucleus

$$-\left(\frac{\mathrm{d}E}{\mathrm{d}t}\right)_{\mathrm{brems}} = 1.435 \times 10^{-40} Z^2 T^{1/2} \bar{g} N N_{\mathrm{e}} \ \mathrm{W\,m^{-3}}$$

The emission co-efficient for free-free transitions is:

$$j_\nu = \frac{8}{3}\left(\frac{2\pi}{3}\right)^{1/2} \frac{Z_i^2 e^6}{m_e^{3/2} c^3 (kT)^{1/2}} g_{ff} n_e n_i \exp -h\nu/kT$$

There must also be a corresponding absorption co-efficient:

$$\begin{aligned}
\kappa_\nu &= j_\nu / B_\nu(T) \qquad \text{(Kirchoff)} \\
&= \frac{4}{3}\left(\frac{2\pi}{3}\right)^{1/2} \frac{Z^2 e^6 n_e n_i g_{ff}}{c m_e^{3/2} (kT)^{3/2} \nu^2} \\
&= 0.1731 \left\{1 + 0.130 \log\left[\frac{T^{3/2}}{Z\nu}\right]\right\} \frac{Z_i^2 n_e n_i}{T^{3/2}\nu^2} \ \mathrm{cm^{-1}}.
\end{aligned}$$

$$\kappa_\nu = 0.1731 \left\{ 1 + 0.130 \log \left[\frac{T^{3/2}}{Z\nu} \right] \right\} \frac{Z_i^2 n_e n_i}{T^{3/2}\nu^2} \ \mathrm{cm}^{-1}.$$

Remembering:

$$B_\nu(T) = \frac{2h\nu^3}{c^2} \frac{1}{\exp h\nu/kT - 1}$$

$$= \begin{cases} \frac{2kT\nu^2}{c^2} & h\nu \ll kT \quad (\mathrm{Rayleigh-Jeans}) \\ \frac{2h\nu^3}{c^2} \exp -h\nu/kT & h\nu \geq kT \quad (\mathrm{Wien}) \end{cases}$$

and substituting:

$$g_{ff} = \frac{3^{1/2}}{\pi} \left\{ \ln \frac{(2kT)^{3/2}}{\pi e^2 Z\nu m_e^{1/2}} - \frac{5\gamma}{2} \right\}$$

$$= 9.77 \left(1 + 0.130 \log \frac{T^{3/2}}{Zv} \right)$$

If: $\tau_\nu \ll 1$
(Optically thin)

The emission that we observe will be

$$\begin{aligned} I_\nu &= I_\nu(0)\exp -\tau_\nu + B_\nu(T)\,(1-\exp -\tau_\nu) \\ &\approx \tau_\nu B_\nu(T) \qquad \text{where} \qquad \tau_\nu = \int \kappa_\nu \mathrm{d}\ell \end{aligned}$$

The logarithmic dependence of the gaunt factor on ν can be approximated as $g_{ff} \propto T_e^{0.15}\nu^{-0.1}$, and we can assume that $n_e \approx n_i$, so we then find that

$$\kappa_\nu \propto T^{-1.35}\nu^{-2.1} n_e^2$$

Therefore

$$I_\nu \propto T^{-0.35}\nu^{-0.1}\int n_e^2 \mathrm{d}\ell, \qquad \text{where} \qquad \int n_e^2 \mathrm{d}\ell = EM$$

$$\begin{aligned} T_b^{ff} &= \frac{I_\nu \lambda^2}{2k} = 5.43\left(\frac{10\,\mathrm{GHz}}{\nu}\right)^2\left(\frac{10^4\,\mathrm{K}}{T_e}\right)^{1/2}\left(\frac{EM}{\mathrm{cm}^{-6}\,\mathrm{pc}}\right) g_{ff}\ \mathrm{K} \\ g_{ff} &\approx 4.69\left(1 + 0.176\ln\left(T_e/10^4\,\mathrm{K}\right) - 0.118\ln\left(\nu/10\,\mathrm{GHz}\right)\right) \end{aligned}$$

If: $\tau_\nu \geq 1$
(Optically thick)

The emission that we observe will be

$$I_\nu = I_\nu(0)\exp -\tau_\nu + B_\nu(T)\,(1-\exp -\tau_\nu)$$
$$\approx B_\nu(T) \quad \text{where} \quad \tau_\nu = \int \kappa_\nu \mathrm{d}\ell$$

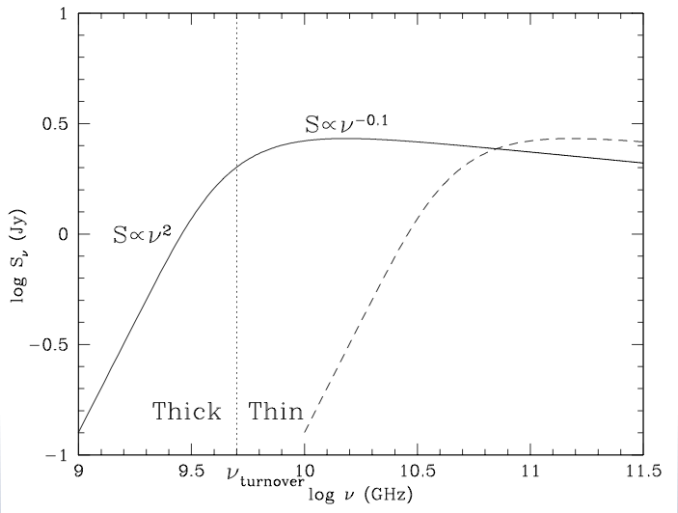

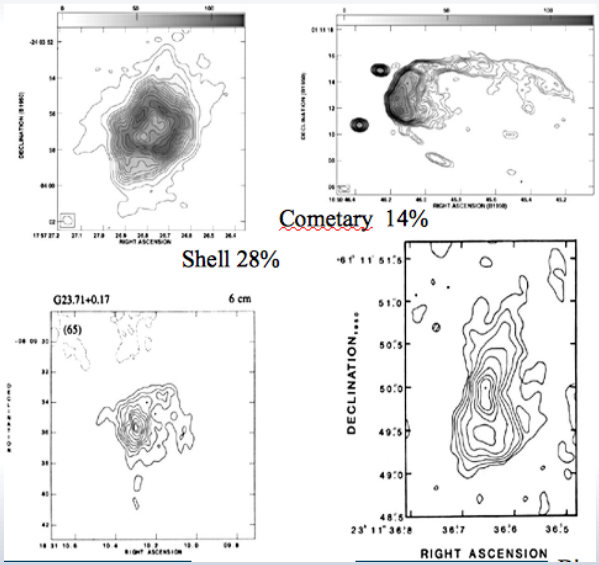

$$\tau_\nu \approx 0.082 T^{-1.35} \nu^{-2.1} \int n_e^2 \mathrm{d}\ell$$
$$\nu_t \approx \left[0.082 T^{-1.35} \int n_e^2 \mathrm{d}\ell\right]^{0.476}$$

Typical physical parameters for UC/HCHII regions are:

Table 4. Quantitative criteria for UCHII and HCHII, summarized from the literature.

Parameter	UCHII	HCHII
Size	<0.1 pc	<0.05 pc
Mean density	$\geq 10^4$ cm^{-3}	$\geq 3\times 10^5$ cm^{-3}
EM	$\geq 10^7$ pc cm^{-6}	$\geq 10^8$ pc cm^{-6}
Recombination linewidth	≤ 40 km s^{-1}	>40 km s^{-1}

(Murphy+ 2010)

with electron temperatures of $T_e \approx 10^4$ K.

If we have much hotter electron gas ($10^7 - 10^8$ K) then the thermal bremsstrahlung gets pushed up into the X-ray regime. e.g. Clusters of Galaxies. . .

$$kT_e \approx \frac{GMm_p}{2R_{eff}} \approx \frac{7}{3}\left(\frac{M}{10^{14}\mathrm{M}_\odot}\right)\left(\frac{R_{eff}}{\mathrm{Mpc}}\right)^{-1} \mathrm{keV}$$

Clusters of Galaxies at High Radio Frequencies

$$L_X \propto \int n_e^2 T_e^\alpha d\ell, \text{ where } \alpha \leq 0.5$$

$$I_{SZ} \propto \int n_e T_e d\ell$$

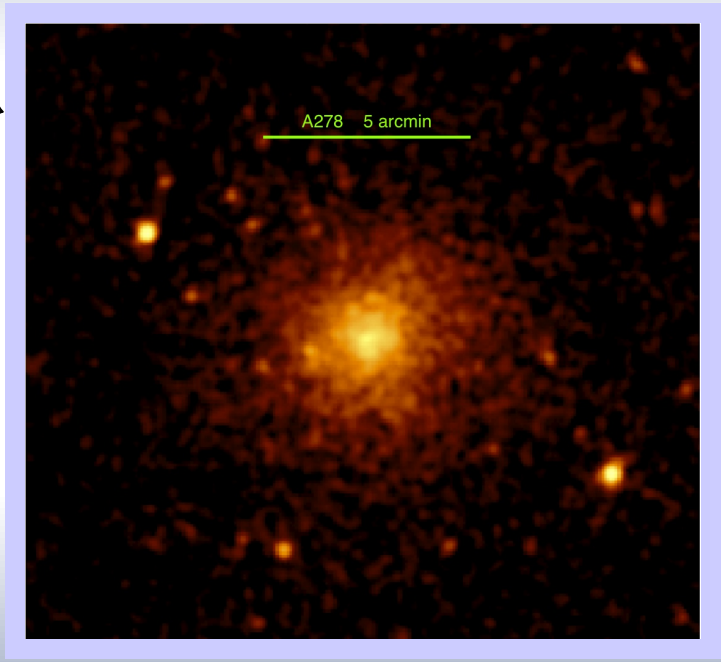

A278: Chandra archive

Clusters of Galaxies at High Radio Frequencies

$$L_X \propto \int n_e^2 T_e^{\alpha} d\ell, \text{ where } \alpha \leq 0.5$$

$$I_{SZ} \propto \int n_e T_e d\ell$$

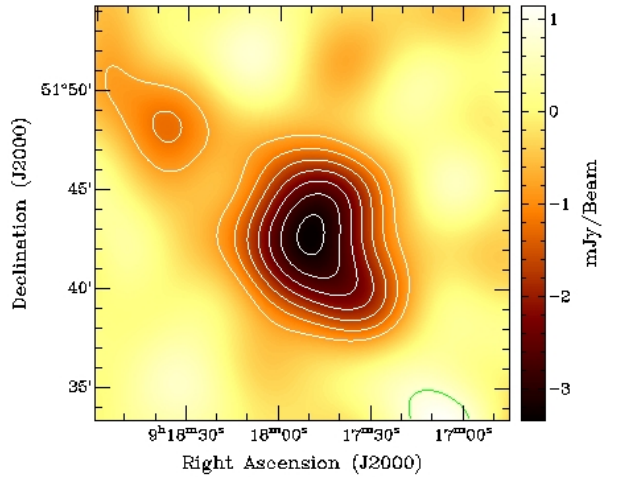

A773: AMI

Outline

1. The Radio Waveband
2. Single Dish Radio Telescopes
3. **High Radio Frequency Science**
   - Thermal Bremsstrahlung
   - The Sunyaev–Zel'dovich (SZ) Effect
4. Radio Interferometry
5. Low Frequency Science
   - Low Frequency Synchrotron Emission
6. Reading List

The SZ effect

Inverse Compton scattering of CMB photons by high energy electrons

The optical depth to scattering through the plasma is:

$$\tau_e = \frac{1}{\lambda_e} = n_e \sigma_T$$

The Comptonization parameter is:

$$y = \frac{k\sigma_T}{m_e c^2} \int n_e T_e \mathrm{d}\ell = \theta_e \tau_e$$

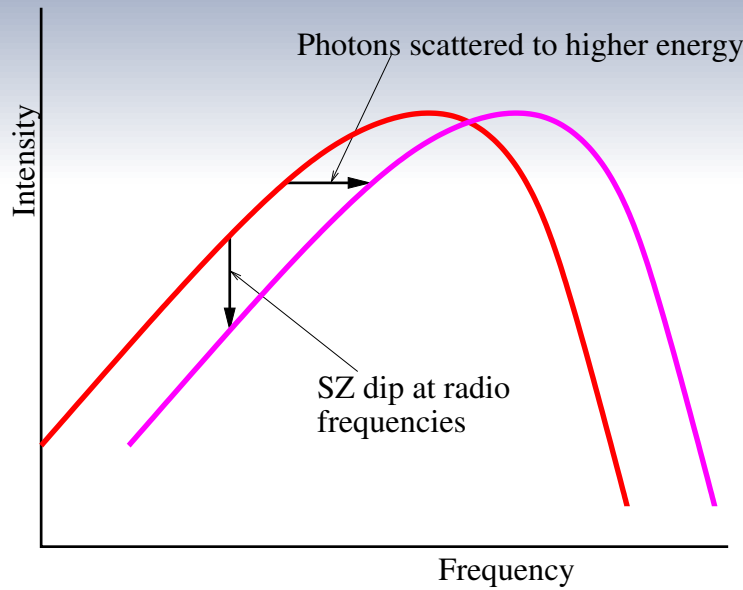

and the change in occupation number of the photons is:

$$\Delta n = xy \frac{\mathrm{e}^x}{(\mathrm{e}^x - 1)^2} \left(x \coth\left(\frac{x}{2}\right) - 4 \right) \quad \text{where} \quad x = \frac{h\nu}{kT_0} \quad \text{(Kompaneets)}$$

The associated change in intensity is:

$$\Delta I = x^3 \Delta n I_0 \quad \text{where} \quad I_0 = \frac{2h}{c^2} \left(\frac{kT_0}{h} \right)^3$$

The SZ effect

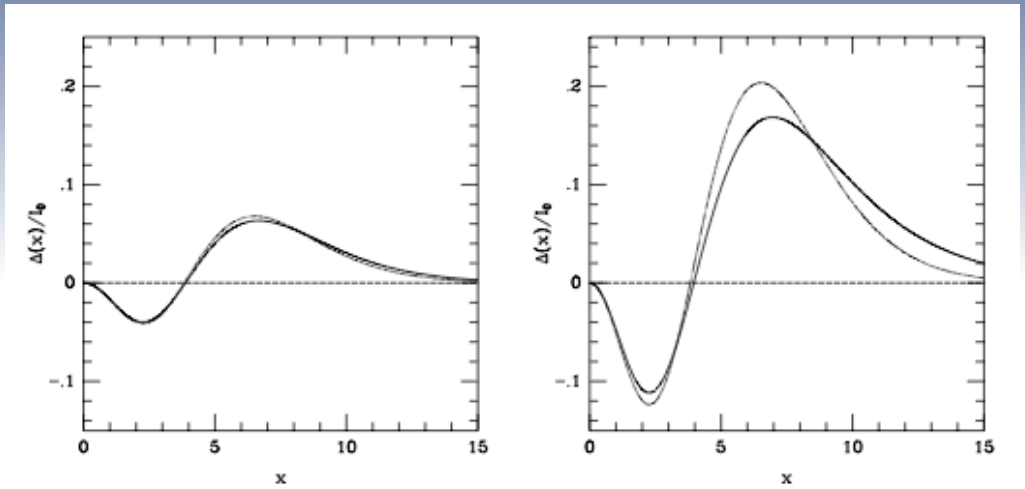

(Birkinshaw 1999)

In the Rayleigh-Jeans region:

$$\frac{\Delta I_\nu}{I_\nu} = -2y$$

The y-parameter is a linear measure of the **pressure** along the line of sight through a cluster of galaxies and therefore (for non-relativistic plasma) the integrated y-parameter:

$$Y = \int y \mathrm{d}\Omega \propto pV$$

provides a direct measure of the internal energy $U = (1/(1-\gamma)pV$ in the cluster gas.

The first SZ detection

- OVRO 40 m dish
- 40 m dish at 20 GHz $\rightarrow$ $\Delta\theta \approx 1.3$ arcmin
- High redshift clusters have sizes of about 1 arcmin
- OVRO 40 m at 20 GHz measures entire galaxy clusters as point sources i.e. in a single beam

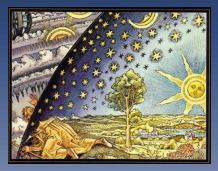

MACS 0744

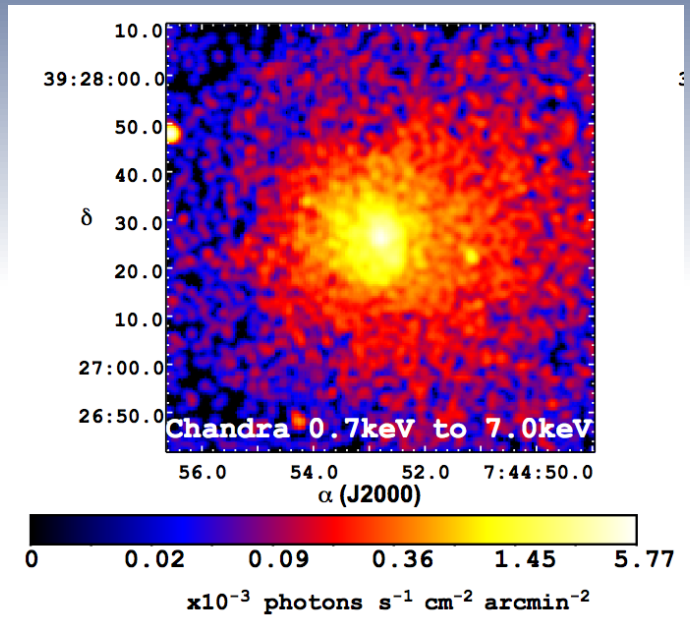

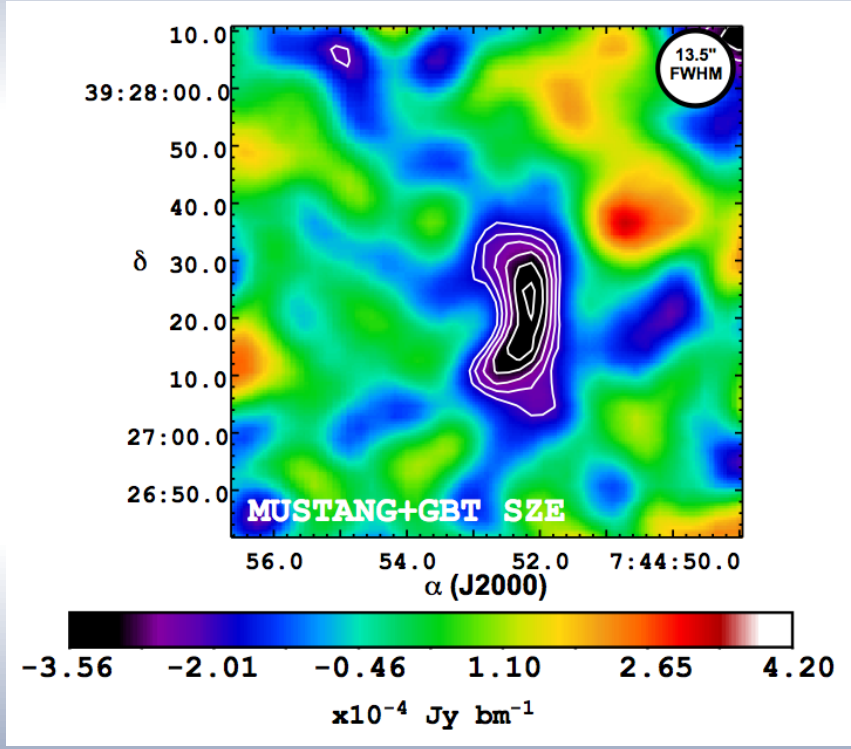

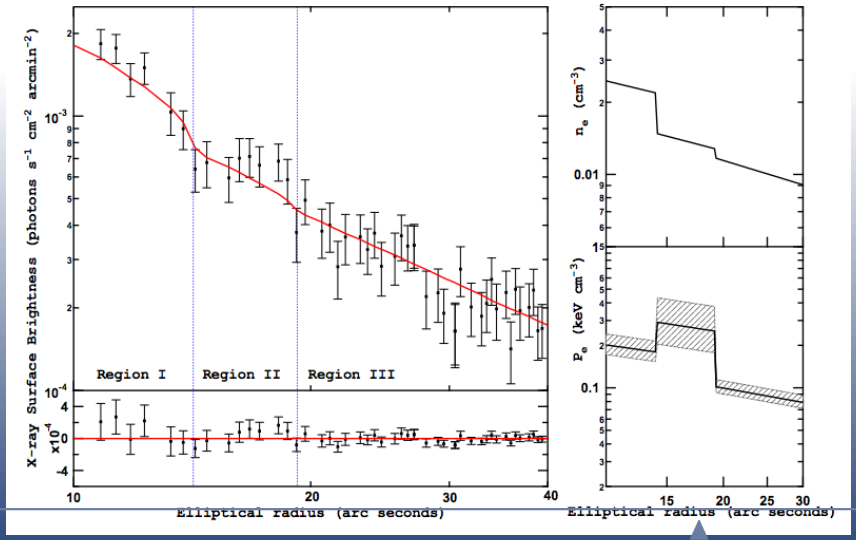

(Korngut+ 2010)

MACS 0744

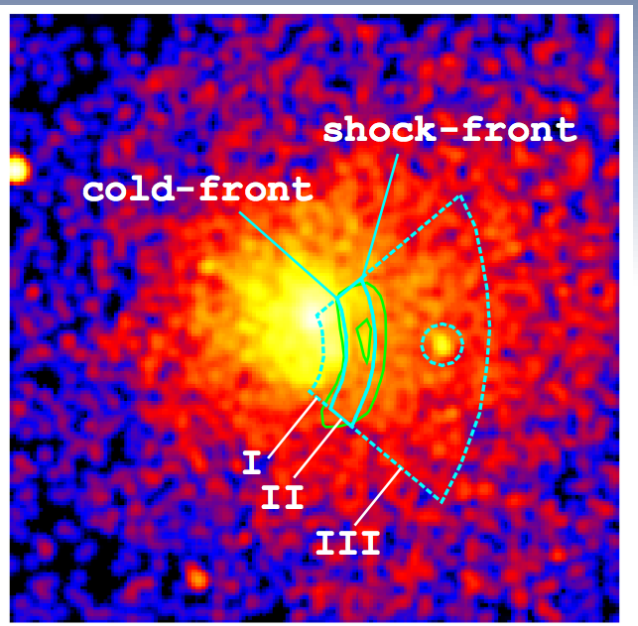

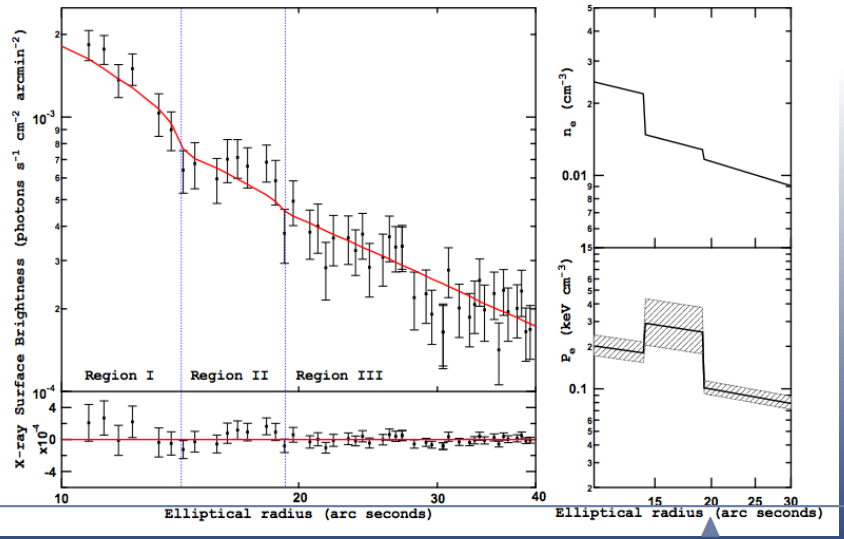

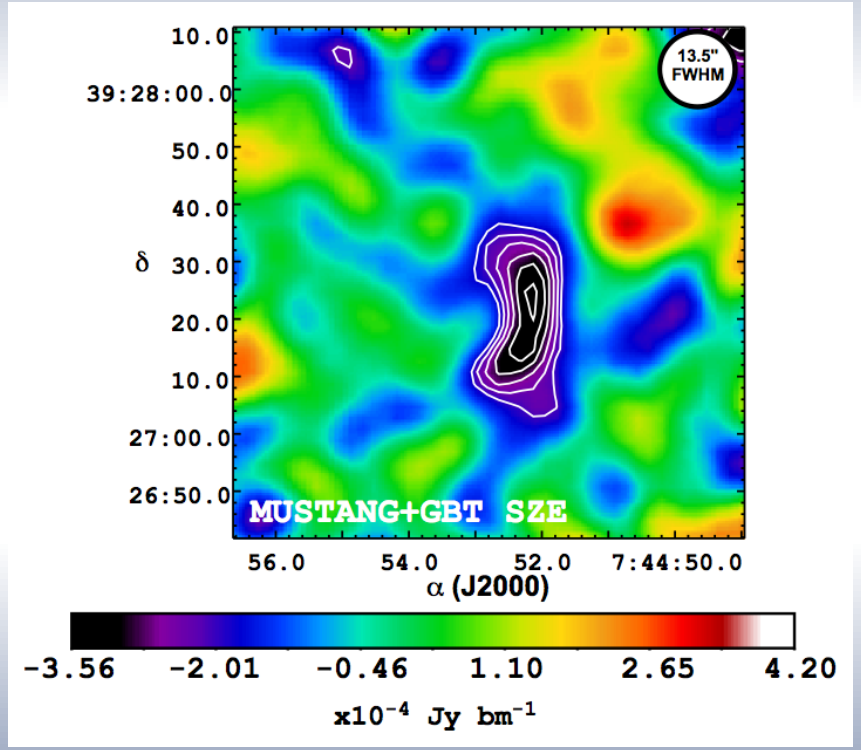

(Korngut+ 2010)

The Resolution Problem

If we tried to observe SZ substructure at 20 GHz with the same telescope:

$$90/20 = 4.5, \qquad 4.5 * 6 = 27 \text{ arcsec}$$

Looking at it another way, to get the same resolution we would need a telescope:

$$D = 4.5 * 100 = 450 \text{ m (!)}$$

This problem is only going to get worse as we go to longer wavelengths. . .

5 MINUTE BREAK

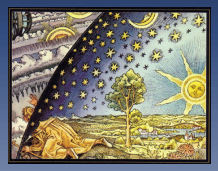

Below the 21 cm line

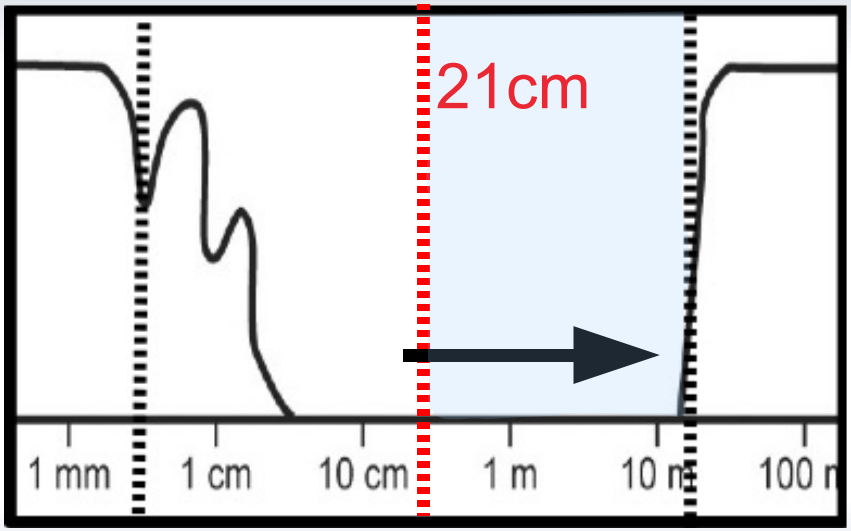

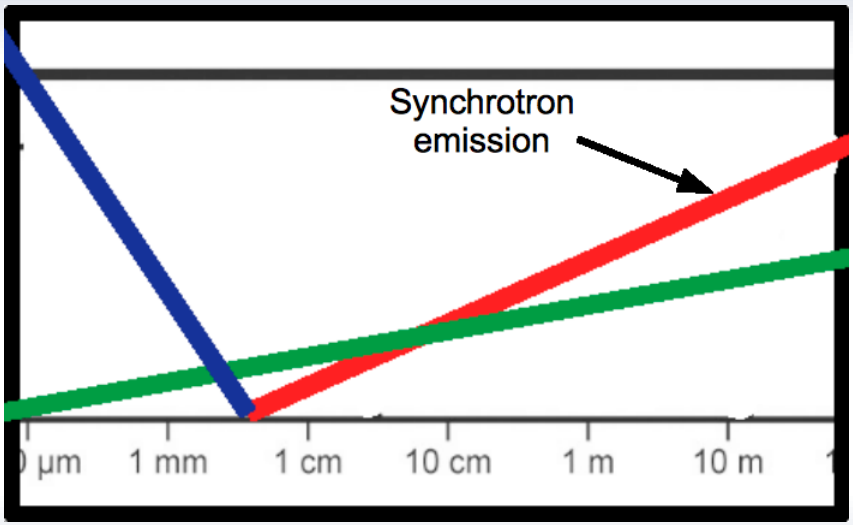

Interferometry

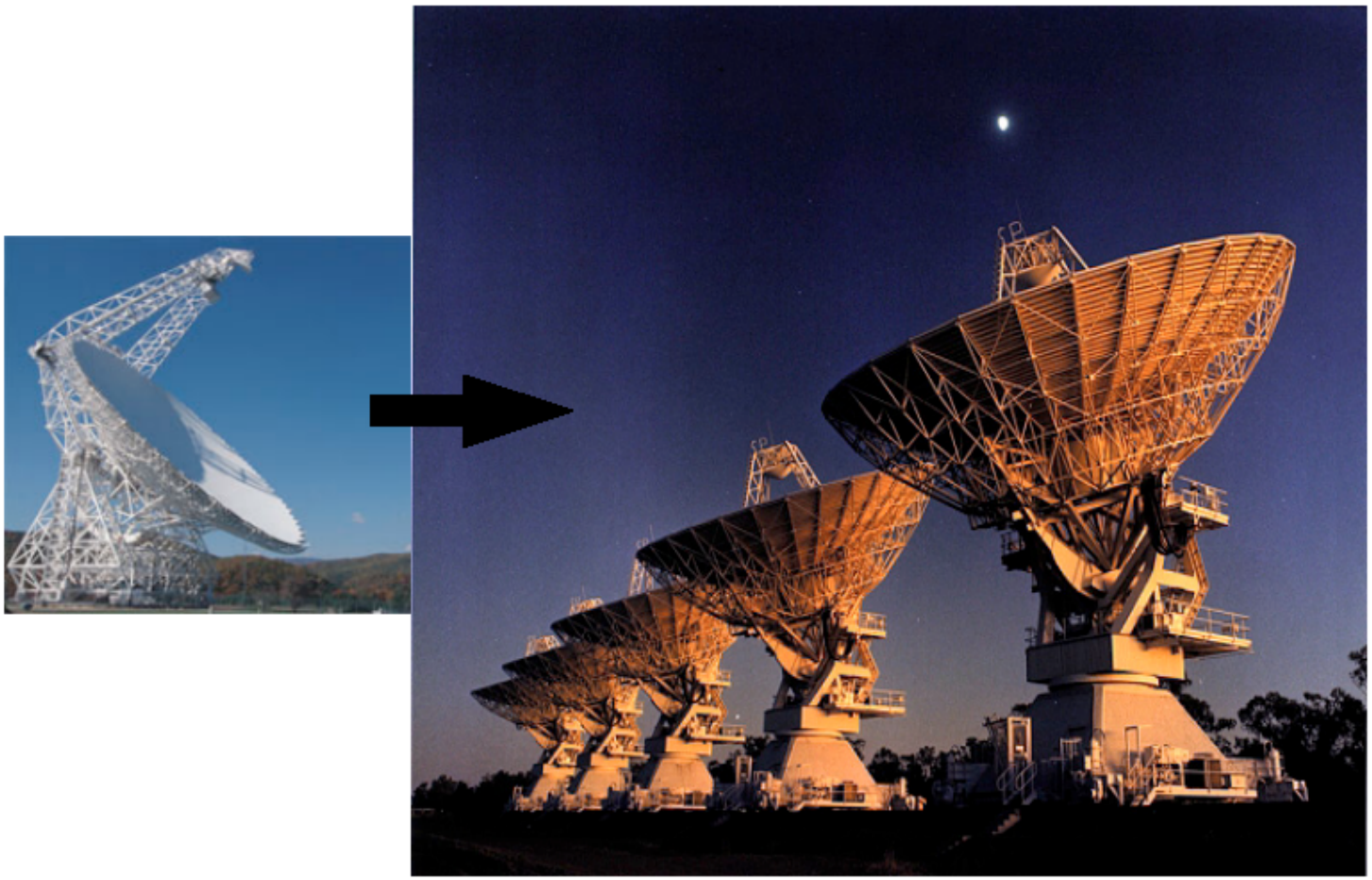

Interferometry

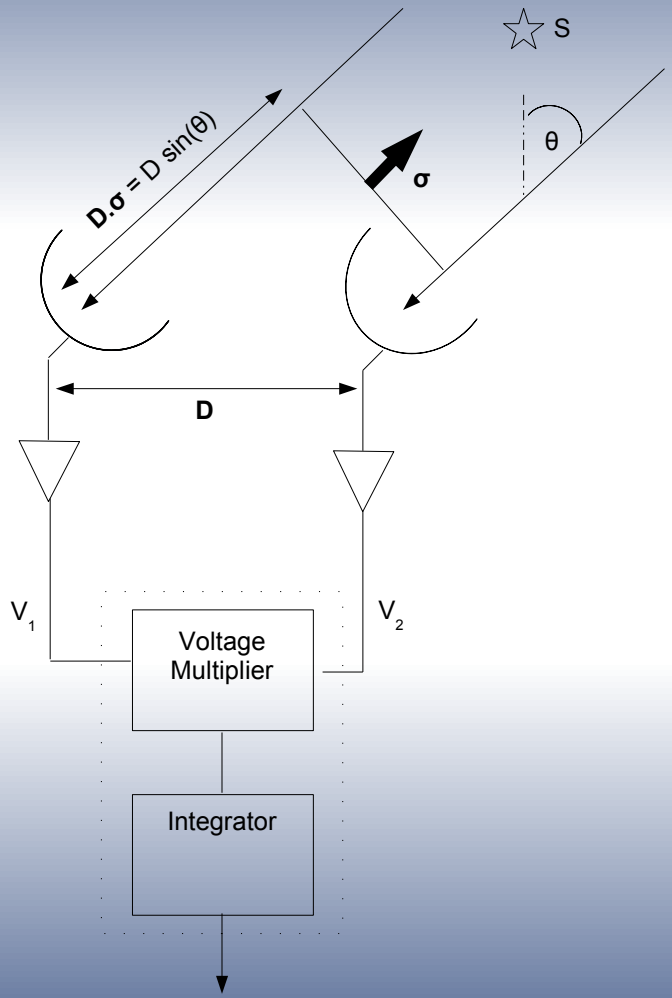

Multiplying the signals from the two antennas

$$F = \sin(2\pi\nu t)\sin(2\pi\nu(t-\tau_g)).$$

The multiplied signals are then integrated over a defined time period. The combination of multiplication and integration is a correlation and the combined voltage multiplier and integrator system is known as the **correlator**. Since the variation of $\nu\tau_g$ will in general be far smaller than νt this multiplication may be approximated by

$$F = \cos(2\pi\nu\tau_g) = \cos\left(\frac{2\pi D\sin\theta}{\lambda}\right).$$

$$F = \cos\left(\frac{2\pi D \sin\theta}{\lambda}\right)$$

These sinusoids are called **fringes** and the fringe phase is defined as

$$\phi = \frac{2\pi D \sin\theta}{\lambda}$$

It varies with source position, θ, as

$$\frac{\mathrm{d}\phi}{\mathrm{d}\theta} = \frac{2}{\pi} D \cos\theta\lambda$$

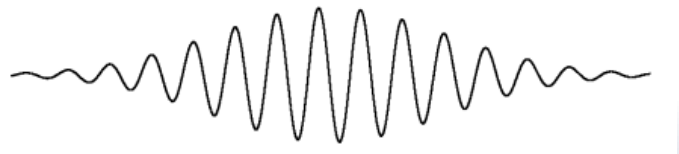

The quantity $D \sin\theta$ is the length of the baseline with length D **projected** onto the plane perpendicular to the direction of observation.

In practice an instrumental time delay τ_{i} will be inserted into the backend of one antenna before multiplication in order to compensate for τ_{g} towards a defined position on the sky. This pre-defined position is known as the **phase center** and will generally, although not necessarily, be aligned with the peak of the aperture illumination function. In interferometry the aperture illumination function is known as the **primary** beam, for reasons which will become apparent. This single instrumental delay, τ_{i}, is only appropriate for one position on the sky; a source offset from the phase center will see a time delay $\tau = \tau_{\mathrm{g}} - \tau_{\mathrm{i}}$.

The rotation of the Earth will cause the position of sources on the sky to be constantly changing with time and it is therefore necessary to constantly update and adjust the instrumental delay, which is often referred to as **path compensation**. If this path compensation is designed such that $\tau_g|_{\theta_0} - \tau_i = 0$ then for a source offset from the phase center, θ_0, by a small amount $\Delta\theta$ the fringe rate will be

$$\begin{aligned} \cos(2\pi\nu_0\tau) &= \cos\left[2\pi\nu_0\left(\frac{D}{c}\sin(\theta_0 - \Delta\theta) - \tau_i\right)\right] \\ &\approx \cos\left[2\pi\sin(\Delta\theta)\nu_0(D/c)\cos(\theta_0)\right]. \end{aligned} \tag{1}$$

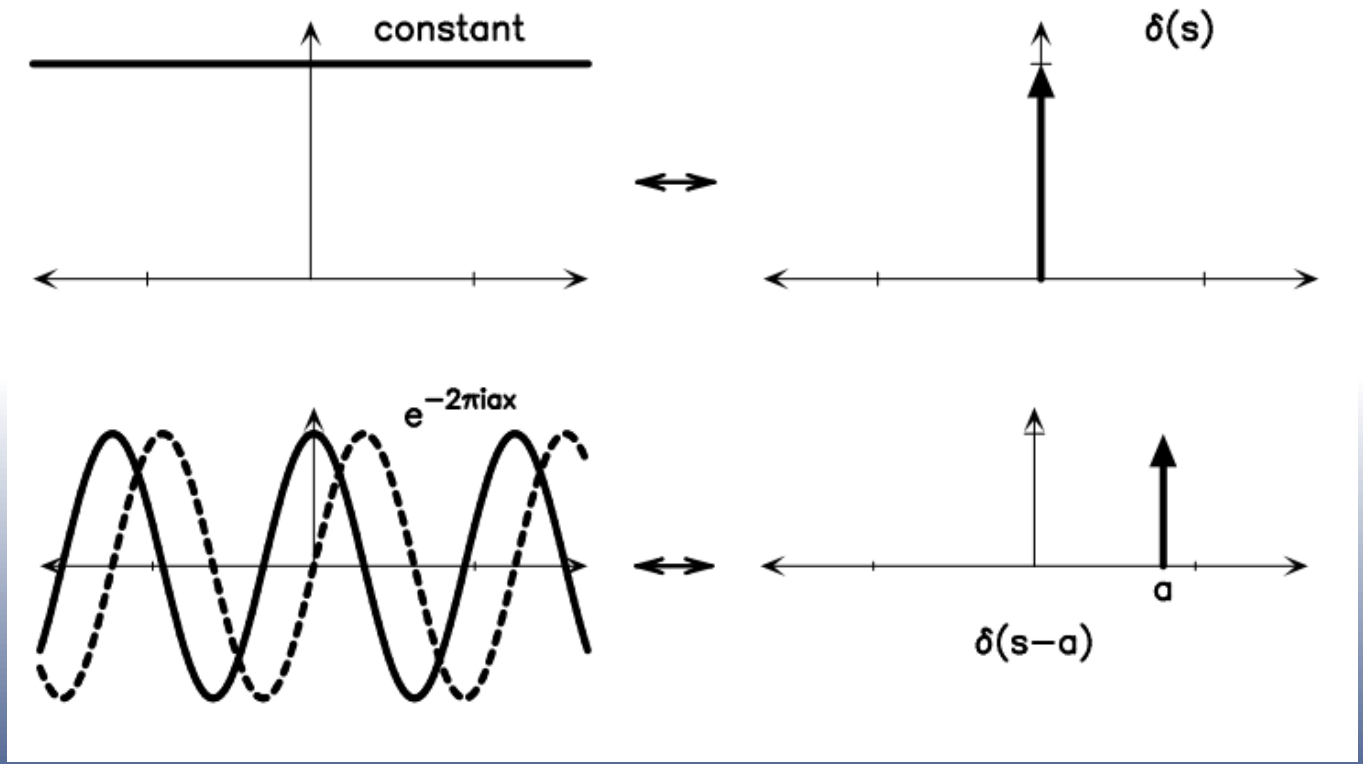

If the integrator has a time constant $2T >> \Delta\nu^{-1}$, the output from the correlator will be the autocorrelation function

$$R(\tau) = \frac{1}{2T}\int_{-T}^{T} V(t)V(t-\tau)dt. \tag{2}$$

This signal will of course be bandlimited by the amplifiers in the telescope system and so, using the Wiener–Khinchin relation[1],

$$R(\tau) = \epsilon(\tau)\cos(2\pi\nu_0\tau), \tag{3}$$

where $\epsilon(\tau)$ is an envelope function determined by the bandpass known as the **delay pattern** and ν_0 is the center of the frequency passband.

[1] The power spectrum of a deterministic signal is the Fourier transform of the autocorrelation of that signal: $|H(\nu)|^2 = \int_{-\infty}^{\infty} R(\tau)e^{-i2\pi\nu\tau}\,d\tau$, and conversely $R(\tau) = \int_{-\infty}^{\infty} |H(\nu)|^2 e^{i2\pi\nu\tau}\,d\nu$.

The argument of this function is written in such a way as to emphasise the contribution from $\nu_0(D/c)\cos(\theta_0)$. This quantity represents the length of the baseline as projected onto the plane normal to the direction to the phase center. It is measured in wavelengths and is interpreted as the **spatial frequency**: u. Consequently we can rewrite Eq. 1 as

$$\cos(2\pi\nu_0\tau) = \cos(2\pi u l) \qquad (4)$$

where $l = \sin(\Delta\theta) \approx \Delta\theta$.
The overall response of the interferometer can therefore be written as

$$R(l) = \int_S \cos\left[2\pi u(l - l')\right] A(l')\epsilon(l')I(l')dl'. \qquad (5)$$

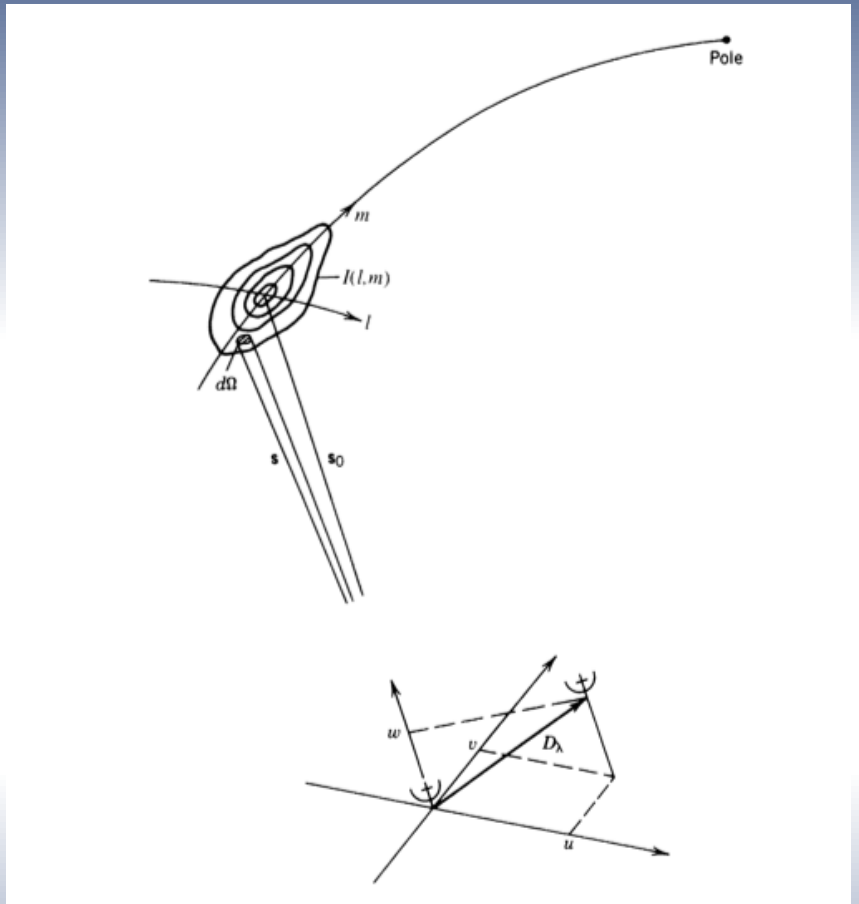

We can now extend the idea of a two element interferometer to a two dimensional synthesis array. Accordingly, we need to exchange our one dimensional notation with a corresponding 2D geometry. For example, our phase centre $\theta_0 \longrightarrow \mathbf{s}_0$. Momentarily neglecting the shape of the bandpass response we may re-write the response of the telescope correlator as

$$R(\mathbf{D}_\lambda, \mathbf{s}_0) = \Delta\nu \int_{4\pi} A(\sigma) I(\sigma) \cos\left[2\pi \mathbf{D}_\lambda \cdot (\mathbf{s}_0 + \sigma)\right] d\Omega. \tag{6}$$

If we define a complex **visibility**, V, as

$$V = |V| e^{i\phi_V} = \int_{4\pi} A(\sigma) I(\sigma) e^{-i2\pi \mathbf{D}_\lambda \cdot \sigma} d\Omega, \tag{7}$$

then we are able to express Eq. 6 as

$$\begin{aligned} R(\mathbf{D}_\lambda, \mathbf{s}_0) &= \Delta\nu \{\cos\left[2\pi \mathbf{D}_\lambda \cdot \mathbf{s}_0\right] \Re\{V\} - \sin\left[2\pi \mathbf{D}_\lambda \cdot \mathbf{s}_0\right] \Im\{V\}\} \\ &= A_0 \Delta\nu |V| \cos\left[2\pi \mathbf{D}_\lambda \cdot \mathbf{s}_0 - \phi_V\right]. \end{aligned} \tag{8}$$

The co-ordinates of σ are generally given as (l, m), where l and m are direction cosines away from the phase center; D_λ is the baseline vector (u, v, w) projected onto the plane normal to the direction of the phase center. We might therefore re-express Eq. 7 as

$$V(u,v,w) = \int_{-\infty}^{\infty}\int_{-\infty}^{\infty} A(l,m)I(l,m)e^{-i2\pi\left[ul+vm+w(\sqrt{1-l^2-m^2}-1)\right]}\frac{dl\,dm}{\sqrt{1-l^2-m^2}}$$

and it is this equation which is most often used to express visibility.

$$V(u,v,w) = \int_{-\infty}^{\infty}\int_{-\infty}^{\infty} A(l,m)I(l,m)e^{-i2\pi\left[ul+vm+w(\sqrt{1-l^2-m^2}-1)\right]}\frac{dl\,dm}{\sqrt{1-l^2-m^2}}$$

The w term in the exponent of Eq. 9 is often neglected since for a restricted range of l and m, as is often the case due to the limited nature of $A(l,m)$, this term becomes negligible.
In these circumstances the visibility equation reduces to a two-dimensional Fourier transform and can be reversed to recover the sky intensity distribution from the measured visibilities:

$$I'(l,m) = \int_{-\infty}^{\infty}\int_{-\infty}^{\infty} V(u,v)e^{i2\pi(ul+vm)}\,du\,dv, \tag{9}$$

where $I'(l,m)$ is the true sky intensity, $I(l,m)$, multiplied by the primary beam and the normalization factor $1/\sqrt{1-l^2-m^2}$.

Aperture Synthesis

In the specific case where the baseline lies exactly east–west, the rotation of the Earth will cause the baseline vector **u** to rotate as a function of time and describe a circle in the *uv* plane with radius $|\mathbf{u}|$. For a perfectly east–west baseline this circle will remain in the plane as the baseline has no component parallel to the Earth's rotation axis, and it was this property that was exploited by the earliest earth rotation aperture synthesis telescopes. By changing the length of the baseline, or by using an array of several different baselines all spaced along an east–west line, it is possible to use the rotation of the Earth to synthesize an aperture much larger than it is practical to engineer.

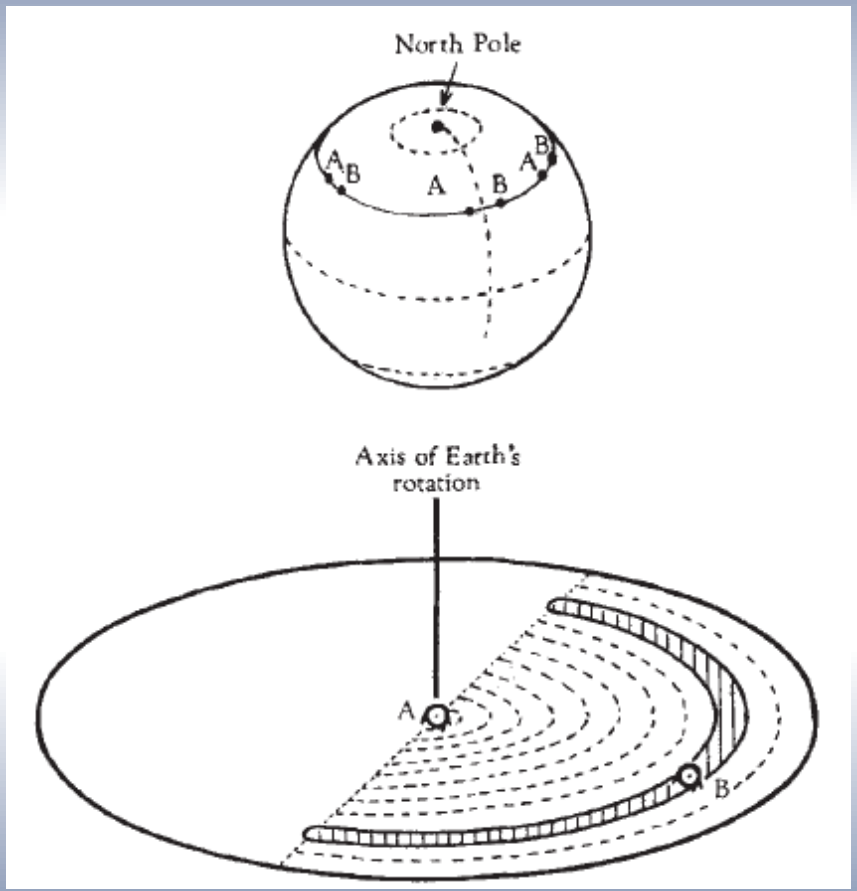

Figure: Geometric description of Earth rotation aperture synthesis (Ryle+ Nature 1962).

One Mile Telescope

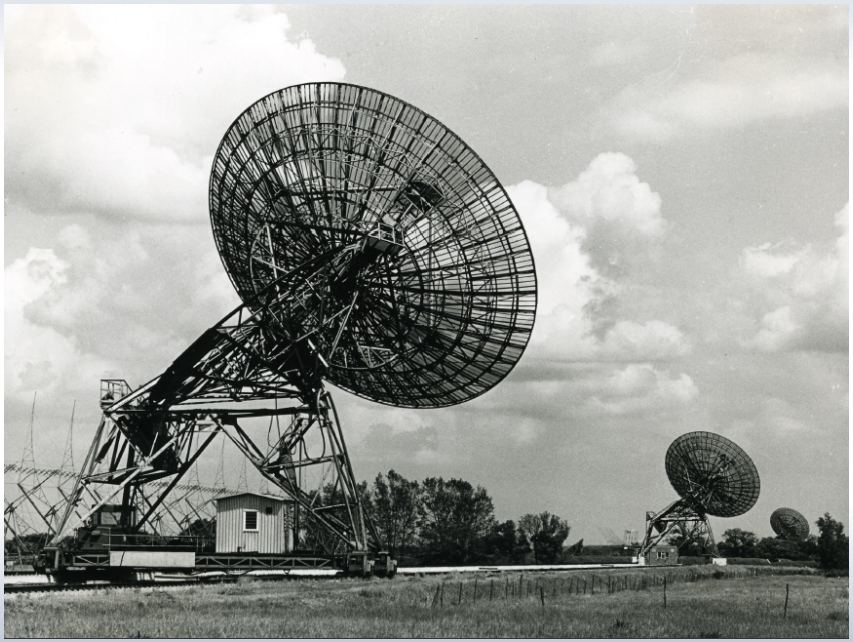

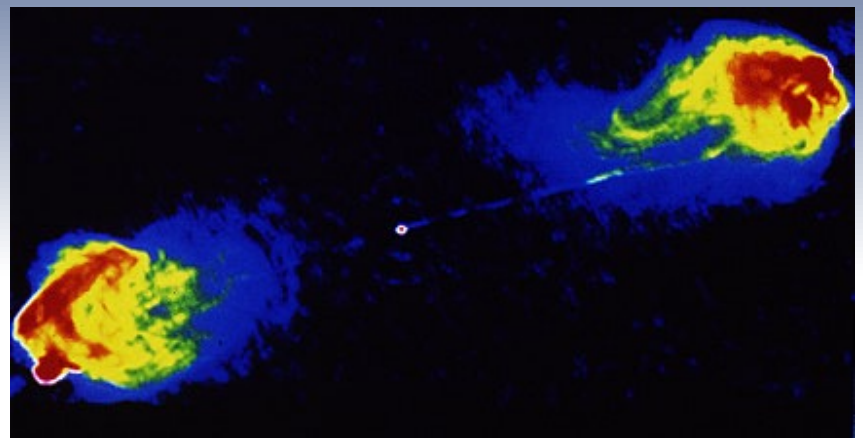

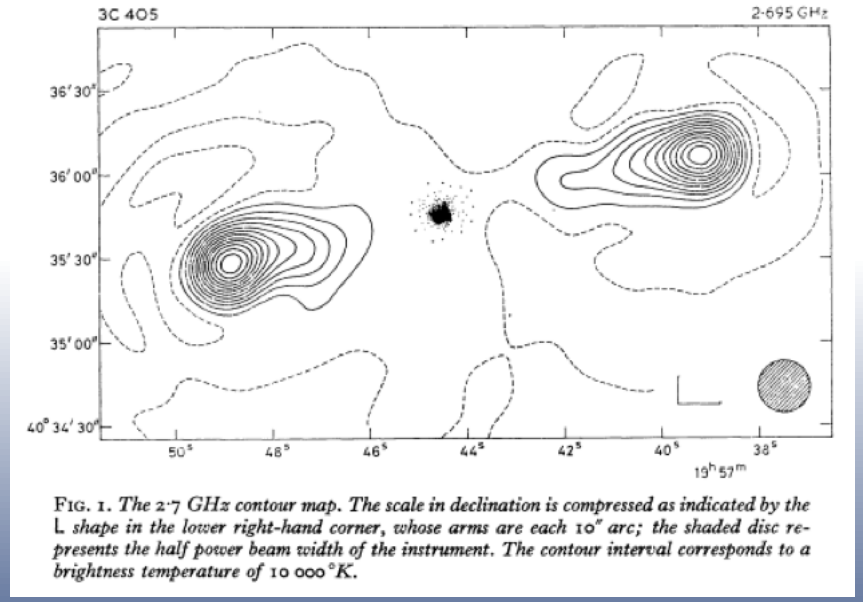

FIG. 1. *The 2·7 GHz contour map. The scale in declination is compressed as indicated by the L shape in the lower right-hand corner, whose arms are each 10″ arc; the shaded disc represents the half power beam width of the instrument. The contour interval corresponds to a brightness temperature of* 10 000 °K.

A baseline is measured in units of wavelength in order to relate it simply to an angular scale, $\Delta\theta \approx D_\lambda^{-1}$. During a synthesis observation the length of the projected baseline will change deterministically as a function of the astronomical pointing direction and local sidereal time.

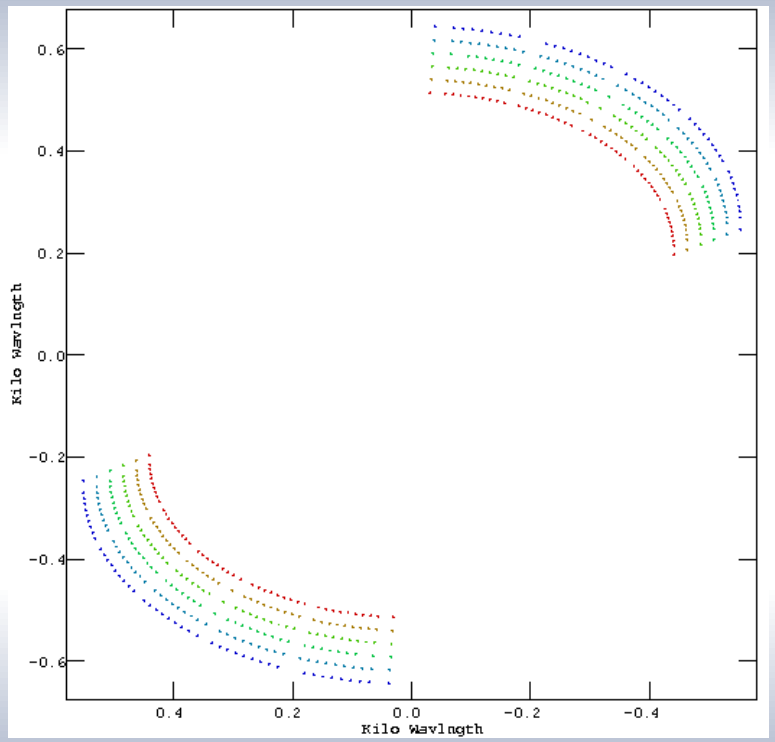

Since the sky signal is intrinisically real the complex amplitude, $V(\mathbf{u})$, received by a baseline will obey the relationship

$$V(-\mathbf{u}) = V^*(\mathbf{u}), \qquad (10)$$

where V^* denotes the complex conjugate of V.

Each δ-fnc component in the sky intensity distribution will contribute a complex exponential to $V(u, v)$

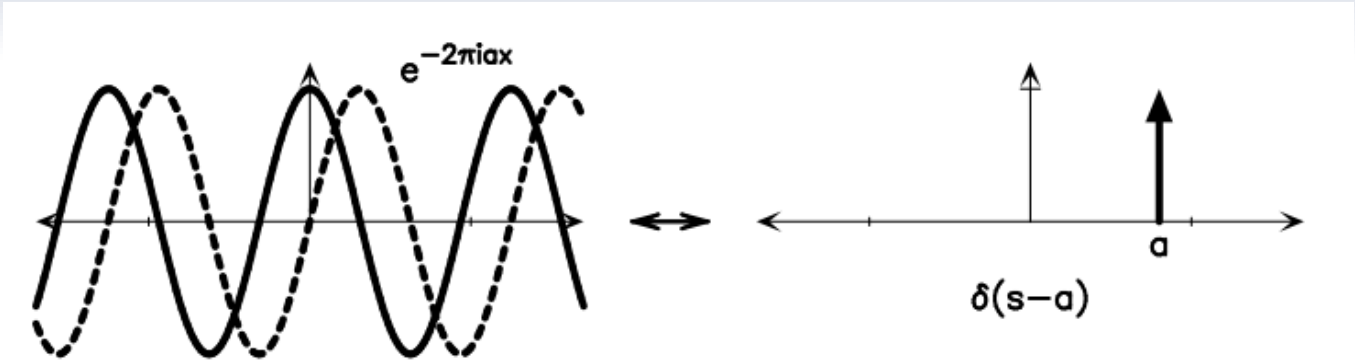

Each δ-fnc component in the sky intensity distribution will contribute a complex exponential to $V(u, v)$

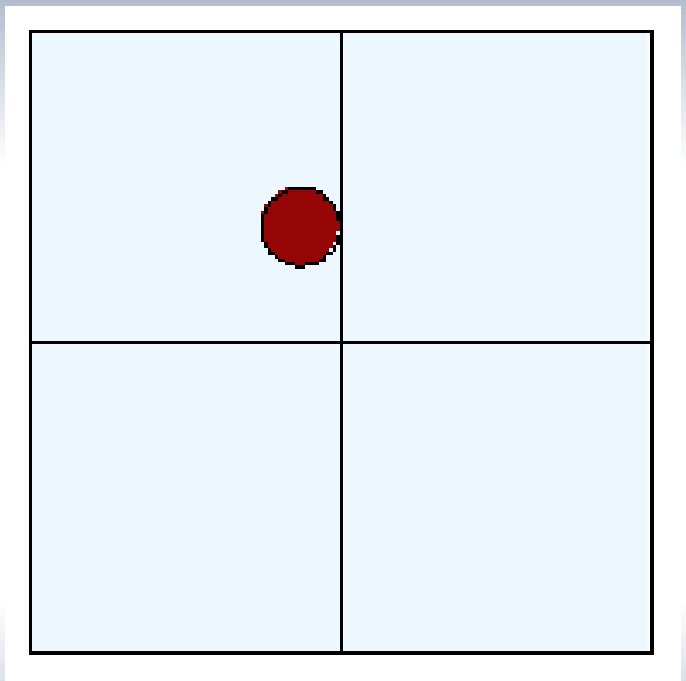

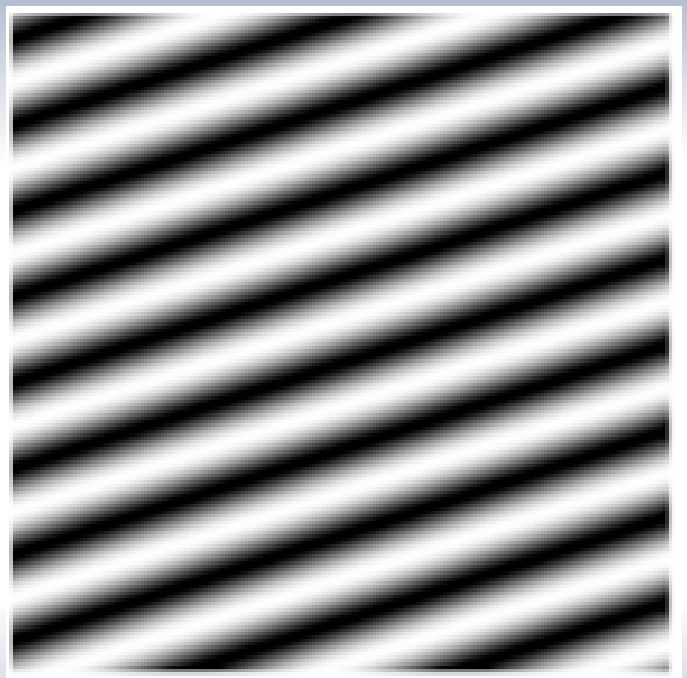

Each δ-fnc component in the sky intensity distribution will contribute a complex exponential to $V(u, v)$

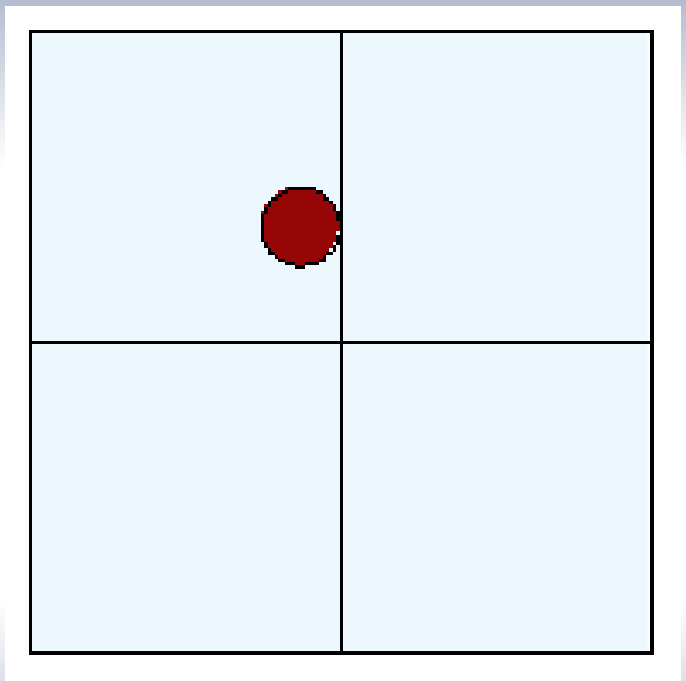

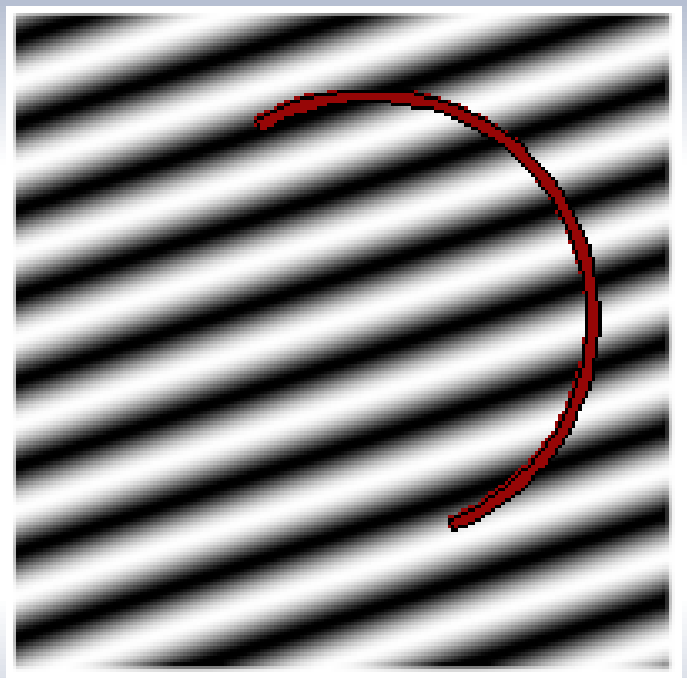

Unlike a true filled aperture, however, it is not possible to measure the zero-spacing flux at the *uv* point $(0, 0)$. This is because the dishes measure only correlated emission and can necessarily be separated only by distances greater than the dish size. A consequence of this is that the total intensity of the sky being measured cannot be found from synthesis measurements, which will always have a total measured flux of zero. A further consequence of the incomplete filling in *uv* space is that the recovered sky is convolved with the Fourier transform of the pattern of the *uv* loci described by the baselines.

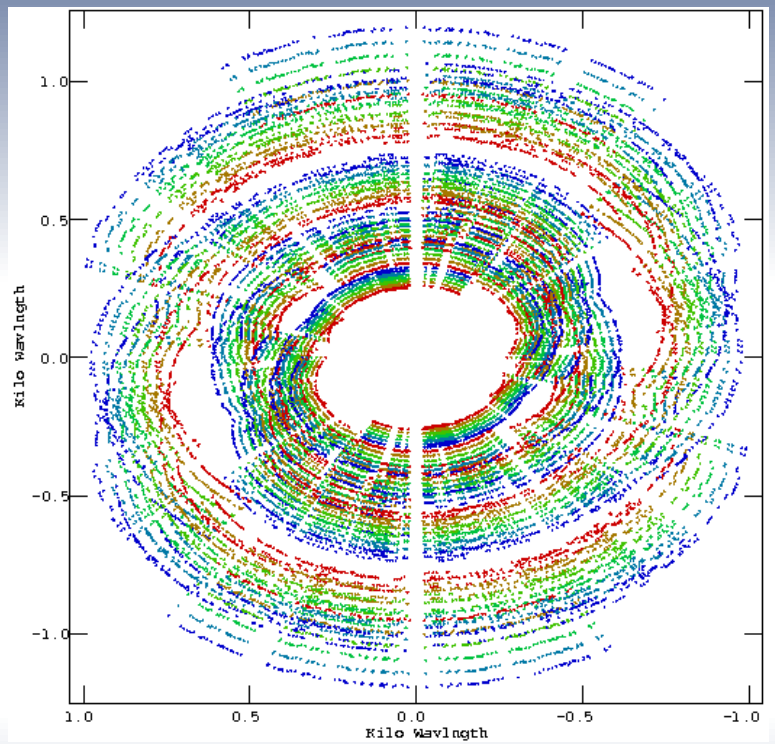

These loci in the *uv* plane may be thought of as a weighting, $W(u, v)$, and their Fourier transform is known as the **synthesized** beam. This distinguishs it from the aperture illumination function, known as the **primary** beam. The relationship between the measured visibilities and the recovered sky intensity can be seen easily using the convolution theorem. Since the true sky intensity distribution $I(l, m)$ is multiplied by the primary beam and its Fourier transform $\tilde{I}(u, v)$ is sampled in *uv* space:

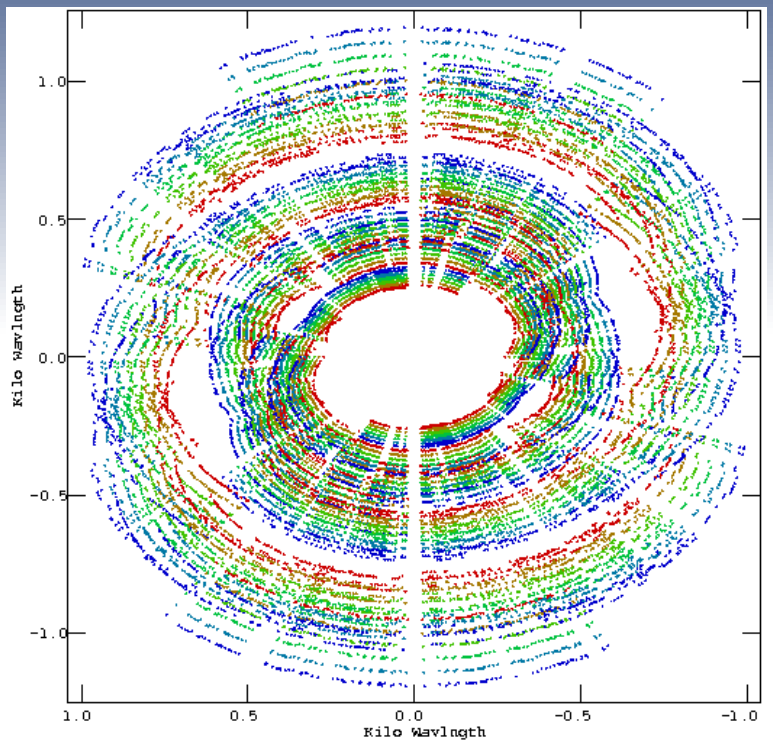

$$[I(l, m) \times A(l, m)] * \tilde{W}(l, m) = \left[\tilde{I}(u, v) * \tilde{A}(u, v)\right] \times W(u, v). \qquad (11)$$

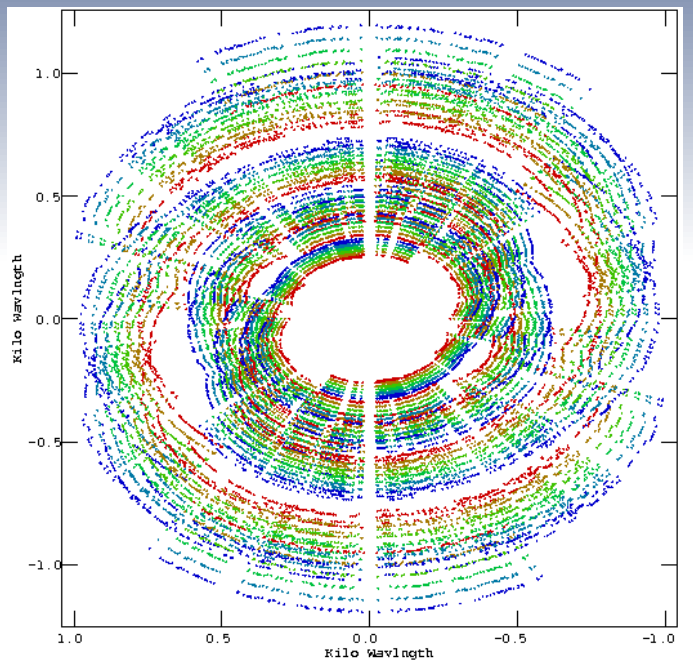
1.0
0.5
0.0
-0.5
-1.0
Kilo Wavlngth
1.0
0.5
0.0
-0.5
-1.0
Kilo Wavlngth

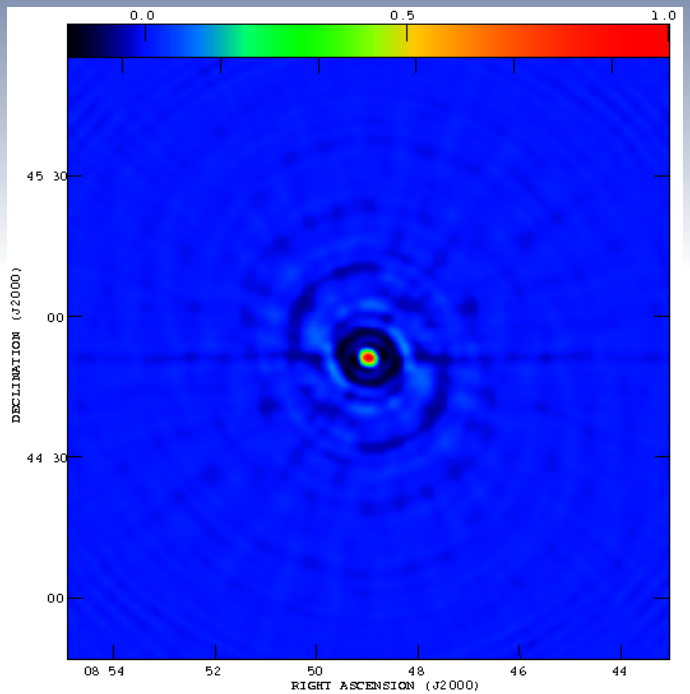
0.0
0.5
1.0
45 30
00
44 30
00
DECLINATION (J2000)
08 54
52
50
48
46
44
RIGHT ASCENSION (J2000)

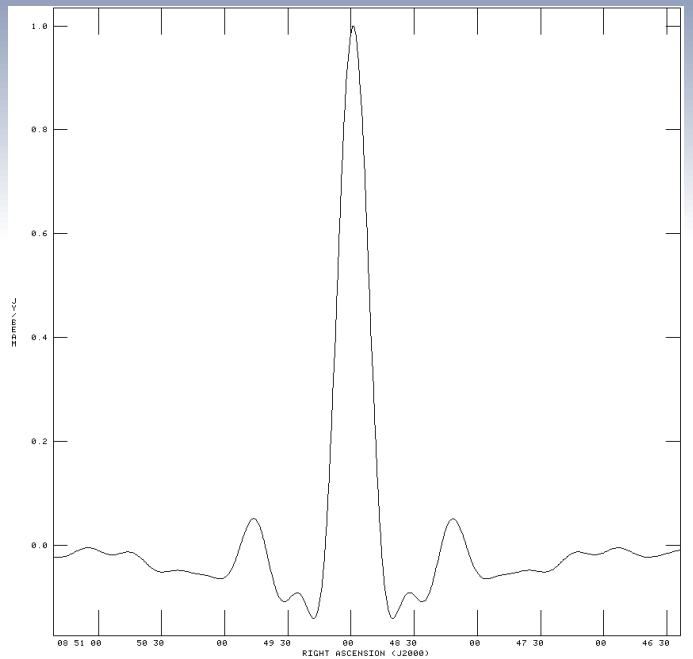
1.0
0.8
0.6
0.4
0.2
0.0
08 51 00
50 30
00
49 30
00
48 30
00
47 30
00
46 30
RIGHT ASCENSION (J2000)

Direct Filtering from Interferometry

Most astrophysical phenomena occur on characteristic scales - why not build a telescope which is preferentially sensitive to those scales?

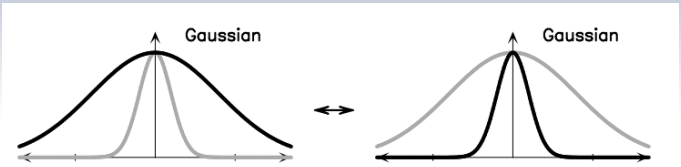

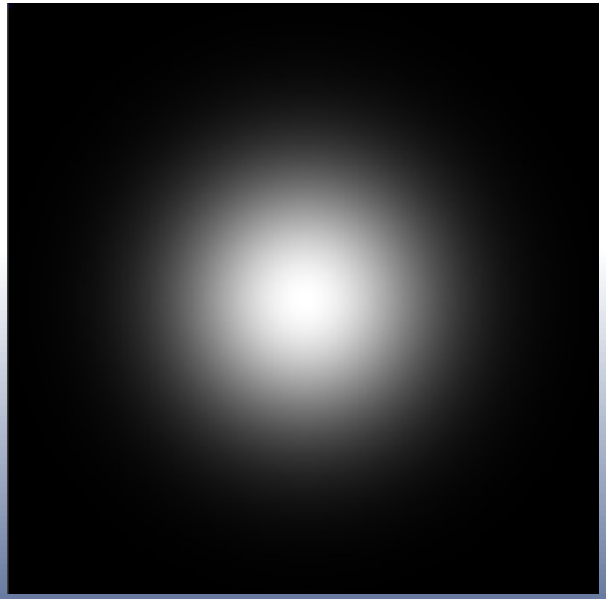

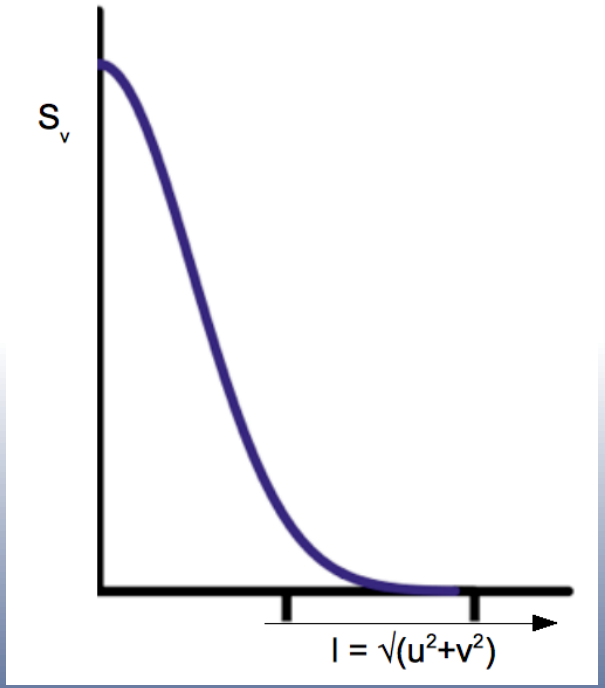

Direct Filtering from Interferometry

Most astrophysical phenomena occur on characteristic scales - why not build a telescope which is preferentially sensitive to those scales?

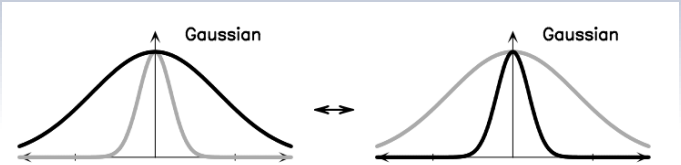

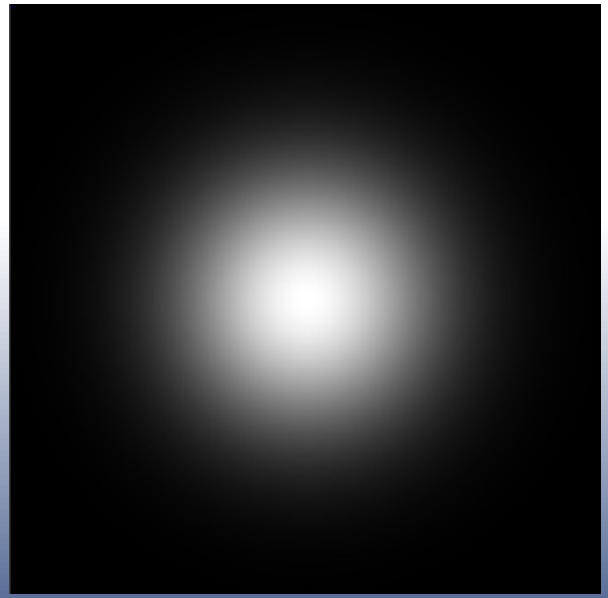

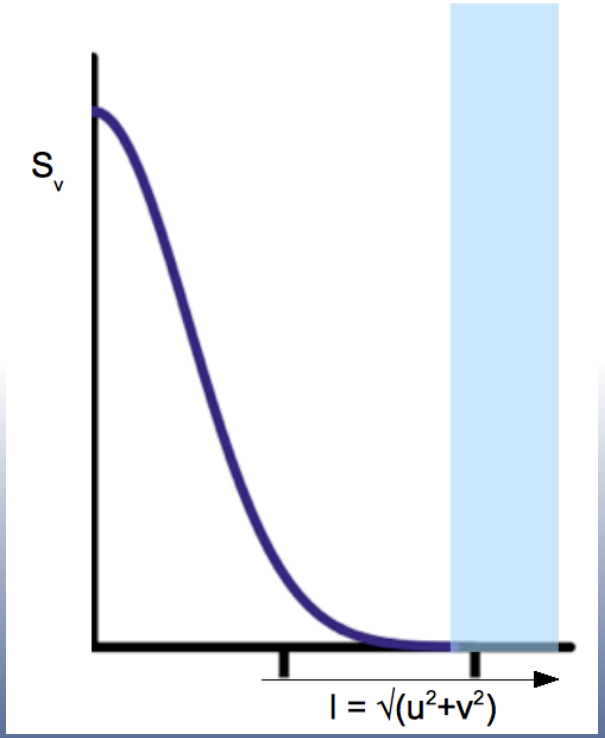

Direct Filtering from Interferometry

Most astrophysical phenomena occur on characteristic scales - why not build a telescope which is preferentially sensitive to those scales?

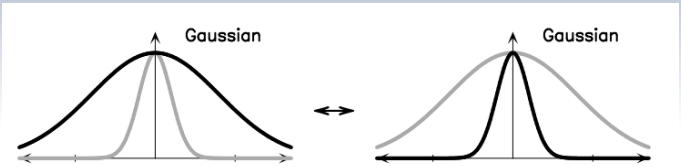

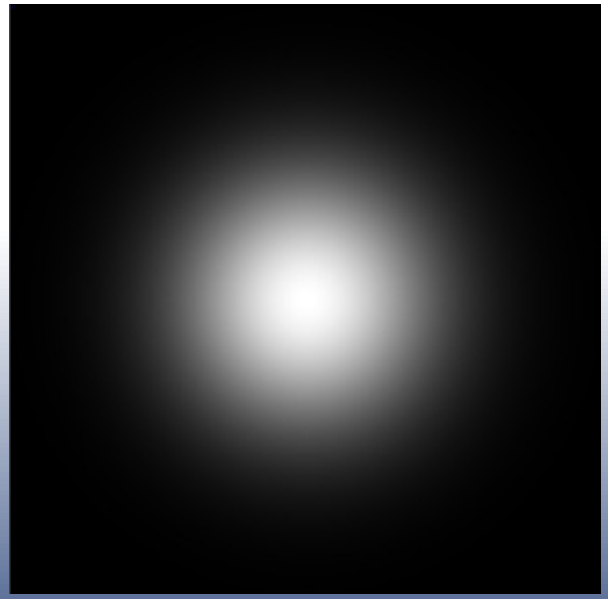

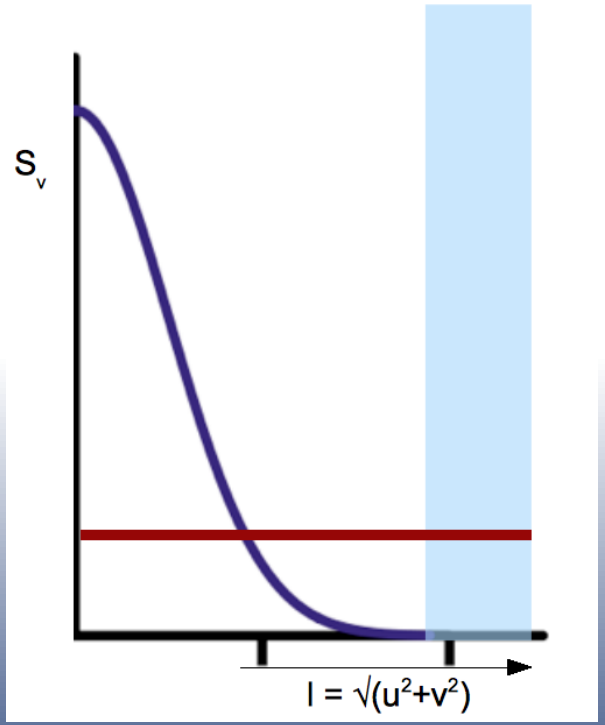

Re-visiting Cluster Detection

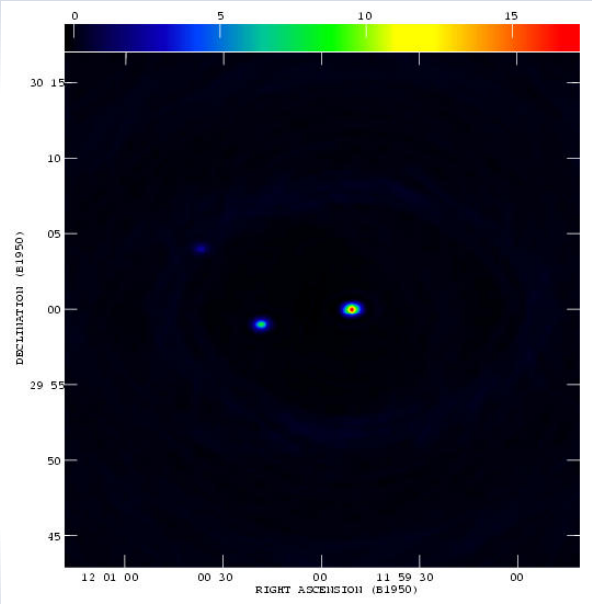

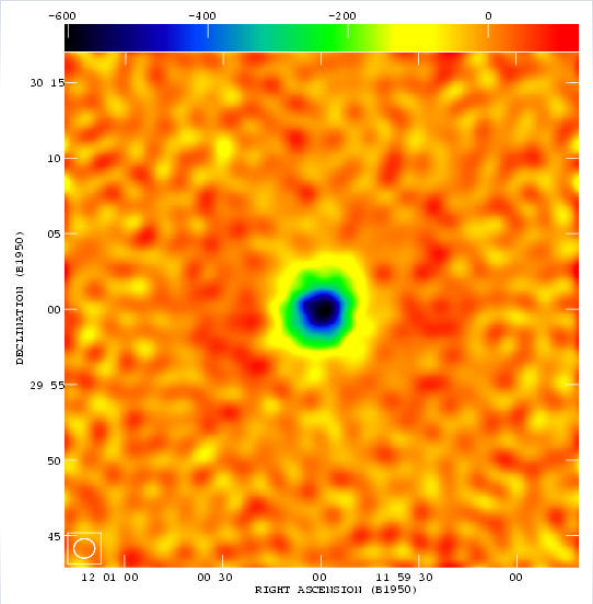

Sensitivity & Resolution

Let's revisit our expression for flux density sensitivity

$$\Delta S = \frac{2kT_{\text{sys}}}{A_{\text{eff}}\sqrt{B\tau}} \Longrightarrow \Delta S = \frac{\sqrt{2}kT_{\text{sys}}}{A_{\text{eff}}\sqrt{N_d(N_d-1)B\tau}}$$

where N_d is the number of dishes in the array, and $N_d(N_d-1)/2$ is the number of baselines.

Our expression for resolution remains similar

$$\Delta\theta \approx \frac{\lambda}{D}$$

but now D is the length of the longest baseline in our array, rather than dish size.

Outline

1. The Radio Waveband
2. Single Dish Radio Telescopes
3. High Radio Frequency Science
   - Thermal Bremsstrahlung
   - The Sunyaev–Zel'dovich (SZ) Effect
4. Radio Interferometry
5. **Low Frequency Science**
   - Low Frequency Synchrotron Emission
6. Reading List

Low frequency synchrotron

Acceleration of ultra-relativistic electrons by a magnetic field

$$-\left(\frac{\mathrm{d}E}{\mathrm{d}t}\right) = \frac{4}{3}\sigma_T c \left(\frac{E}{m_e c^2}\right)^2 \frac{B^2}{2\mu_0}$$

The emission from a population of electrons with a power-law distribution of energies ($N(E)\mathrm{d}E \propto E^{-p}\mathrm{d}E$) therefore depends on the magnetic field strength

$$I_\nu \propto B^{(p+1)/2}\nu^{(p-1)/2} \qquad \text{where} \qquad (p-1)/2 = \alpha \quad \text{(spectral index)}$$

$$\begin{aligned} I_{\mathrm{syn}} &\propto \nu^{-\alpha} B^{\alpha+3} \\ T_{\mathrm{b,syn}} &\propto \nu^{-(\alpha+2)} B^{\alpha+3} \end{aligned}$$

Assuming equipartition:

$$\mathbf{B_{min} \propto \nu^{(\alpha+2)/(\alpha+3)}}$$

$$\Downarrow$$

10× lower frequency = 5× lower $\mathbf{B_{min}}$

Low frequency synchrotron

The extent of synchrotron sources is limited by the propagation speed and the lifetime of the primary electrons - which is limited by synchrotron and inverse-Compton losses

$$t_{1/2} = 1.59 \times 10^9 \frac{B^{1/2}}{B^2 + B_{CMB}^2} \left[\left(\frac{\nu}{\mathrm{GHz}} \right) (1+z) \right]^{-1/2}$$

$$\text{where} \quad B_{CMB} = 3.25(1+z)^2 \, \mu\mathrm{G} \tag{12}$$

B_{CMB} is the **equivalent** magnetic field strength of the CMB at redshift z assuming equipartition.

$$\dot{E}_{syn} \propto -u_{mag} E^2$$
$$\dot{E}_{IC} \propto -u_{rad} E^2$$

$$u_{mag} = \frac{B^2}{8\pi}$$
$$u_{rad} \propto T_{CMB}^4$$

Low frequency synchrotron

The lifetime of electrons suffering synchrotron losses therefore increases with decreasing frequency - and decreasing magnetic field strength

$$t_{syn} = 1.1 \times 10^9 \left(\frac{\nu}{\mathrm{GHz}}\right)^{-0.5} \left(\frac{B}{\mu\mathrm{G}}\right)^{-1.5} \mathrm{yr}$$

In magnetic fields weaker than B_{CMB} the electron lifetime is limited by inverse Compton losses on CMB photons. At $B < 1\ \mu$G there are purely inverse Compton losses and the dependence of the lifetime on magnetic field strength reverses sign

$$t_{syn} = 1.0 \times 10^8 \left(\frac{\nu}{\mathrm{GHz}}\right)^{-0.5} \left(\frac{B}{\mu\mathrm{G}}\right)^{0.5} \mathrm{yr}$$

Consequently synchrotron electrons have a maximum lifetime when the magnetic field strength is $B \approx 3\ \mu$G

Low frequency synchrotron

The size of synchrotron emitting sources is also determined by the propagation speed of the CR electrons. In turbulent magnetic fields CRs propagate by diffusion with a diffusion speed = Alfvén speed.

$$\begin{aligned} v_A &= \frac{B}{\sqrt{\mu_0 \rho}} \\ &= \frac{B}{\sqrt{\mu_0 \sum n_i m_i}} \\ &\approx 2.18 \left(\frac{n_e}{\mathrm{cm}^{-3}}\right)^{-0.5} \left(\frac{B}{\mu\mathrm{G}}\right) \mathrm{km\,s}^{-1} \end{aligned}$$

i.e. in a typical galaxy halo with $n_e \simeq 10^{-3}\,\mathrm{cm}^{-3}$, $v_A \simeq 70(B/\mu\mathrm{G})\,\mathrm{km\,s}^{-1}$.

At high radio frequencies synchrotron losses limit emission to ≈1 kpc from it's source.

However, with $v_A \simeq 70(B/\mu\mathrm{G})\,\mathrm{km\,s^{-1}}$ a synchrotron electron radiating at 50 MHz can propagate

$$L \simeq 330\left(\frac{B}{\mu\mathrm{G}}\right)^{0.5}\ \mathrm{kpc} \qquad B \geq 3\,\mu\mathrm{G}$$

$$L \simeq 30\left(\frac{B}{\mu\mathrm{G}}\right)^{1.5}\ \mathrm{kpc} \qquad B \leq 3\,\mu\mathrm{G}$$

At $B \approx 3\,\mu$G (maximum lifetime) a propagation length of **200 kpc** is expected.

$\Longrightarrow$ synchrotron emitting regions are much **bigger** at low frequencies

NGC 253

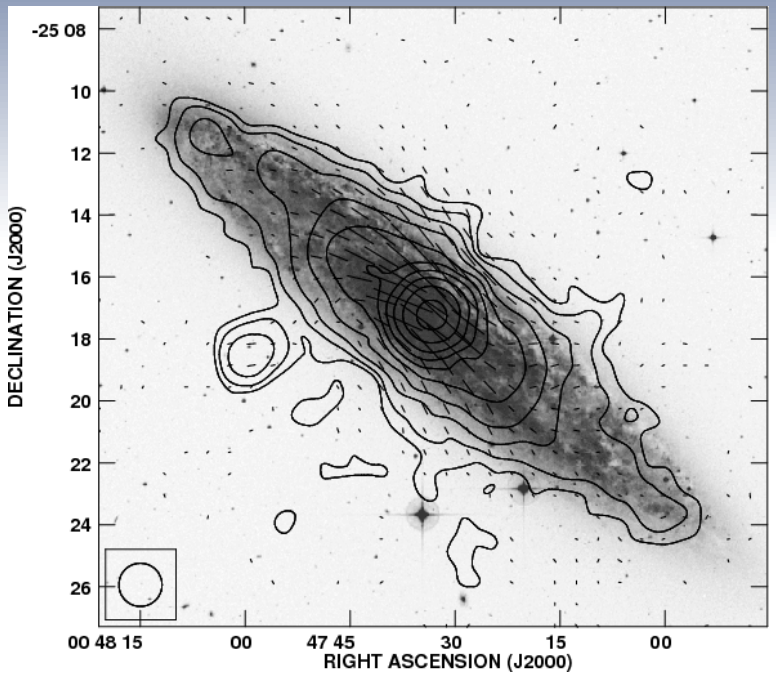

$\lambda = 3.6\,\mathrm{cm}$ (8.5 GHz)

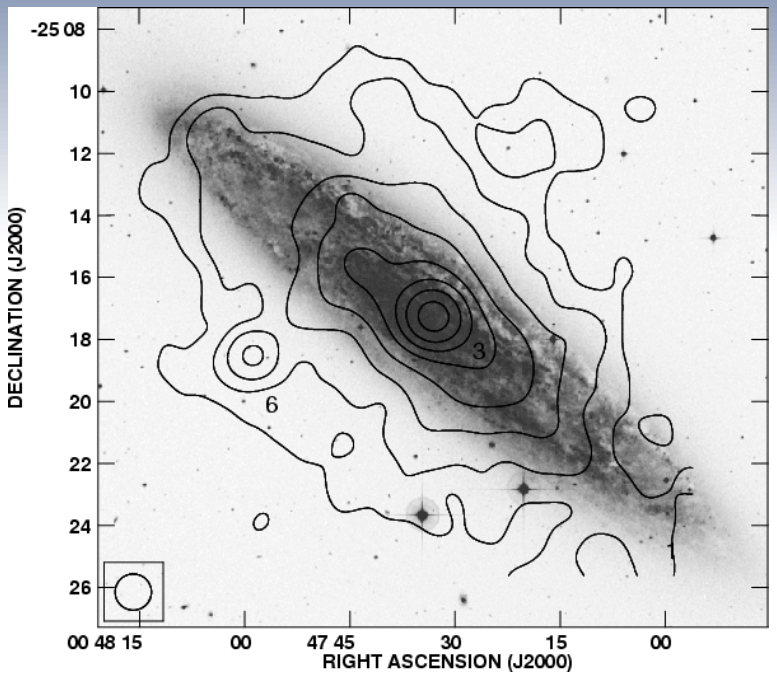

$\lambda = 90\,\mathrm{cm}$ (345 MHz)

(Heesen+ 2009)

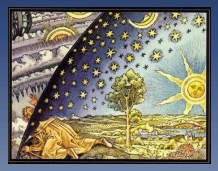

Dipole Arrays

Dipole Arrays

The reception pattern of a dipole is a torus

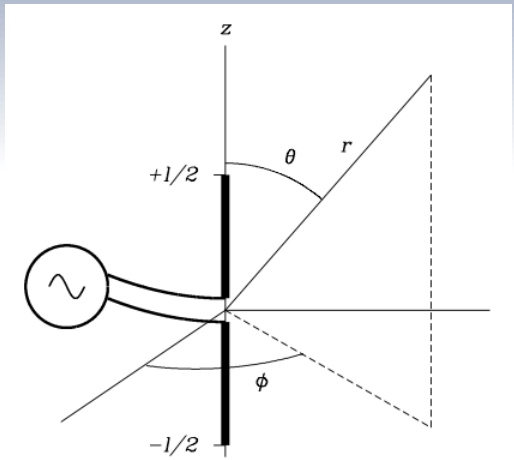

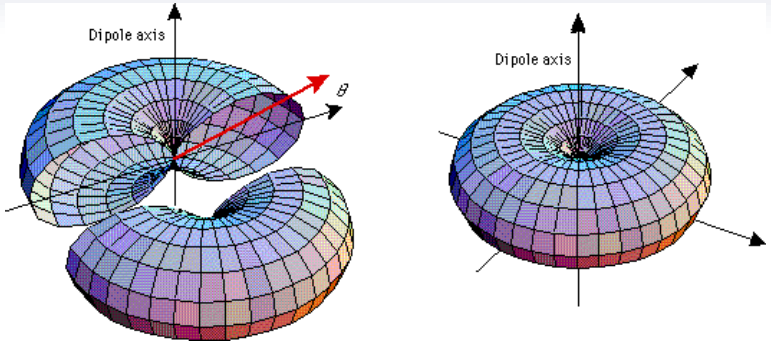

We can alter the directionality of the antenna by applying additional phase

$$f(l) = \int g(u) \mathrm{e}^{-i2\pi ul} \mathrm{d}u \quad u = x/l$$

$$f(l-a) = \int g(u) \mathrm{e}^{-i2\pi au} \mathrm{e}^{-i2\pi ul} \mathrm{d}u$$

Dipole Arrays

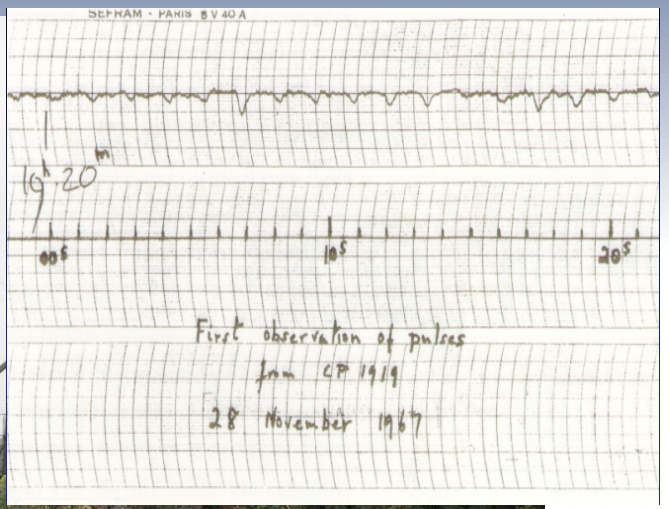

Dipole Arrays

Phasing up an array of dipoles to look in a single direction is known as beam-forming.

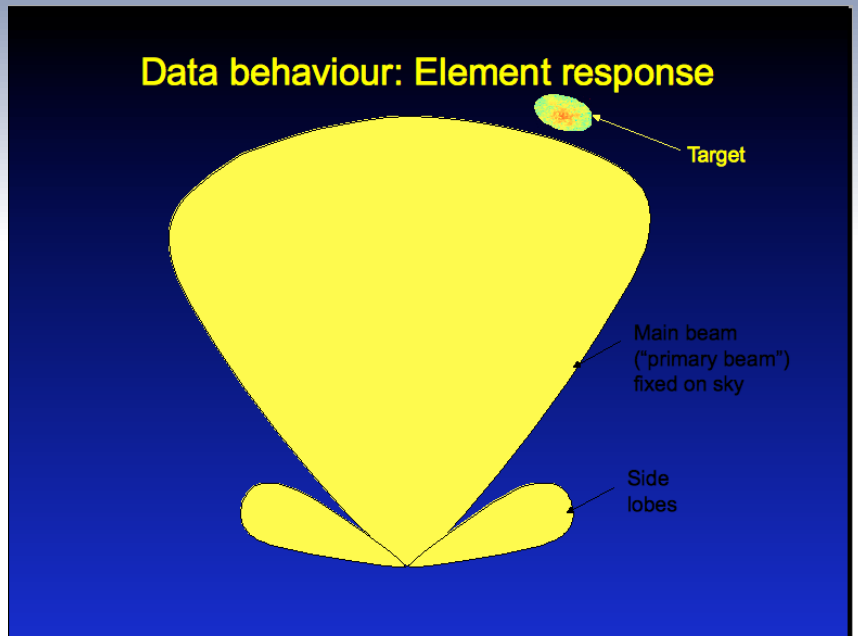
Data behaviour: Element response
Target
Main beam
("primary beam")
fixed on sky
Side
lobes

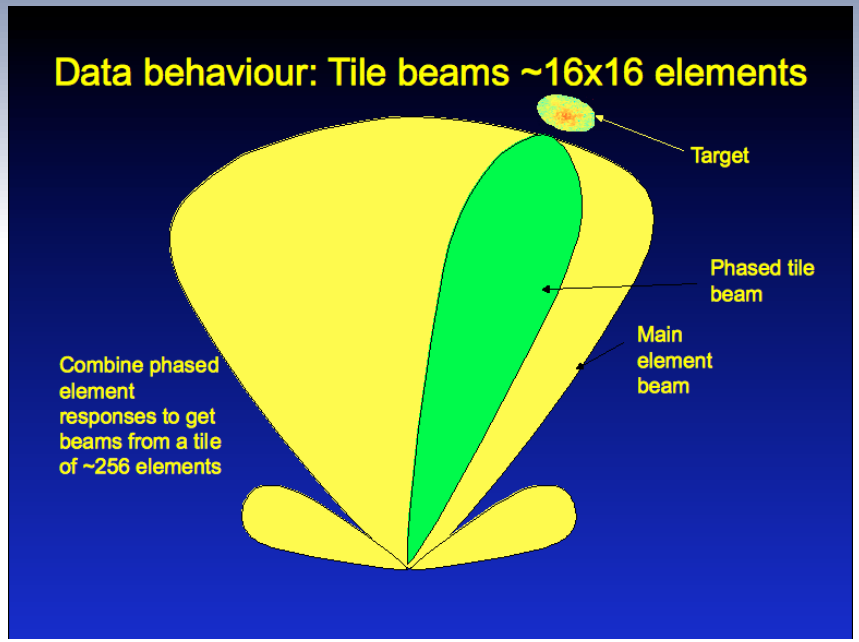
Data behaviour: Tile beams ~16x16 elements
Target
Phased tile
beam
Main
element
beam
Combine phased
element
responses to get
beams from a tile
of ~256 elements

Dipole Arrays

Once you have phased up a small array of dipoles (a station) you can then connect that station to another station interferometrically.

3C61.1

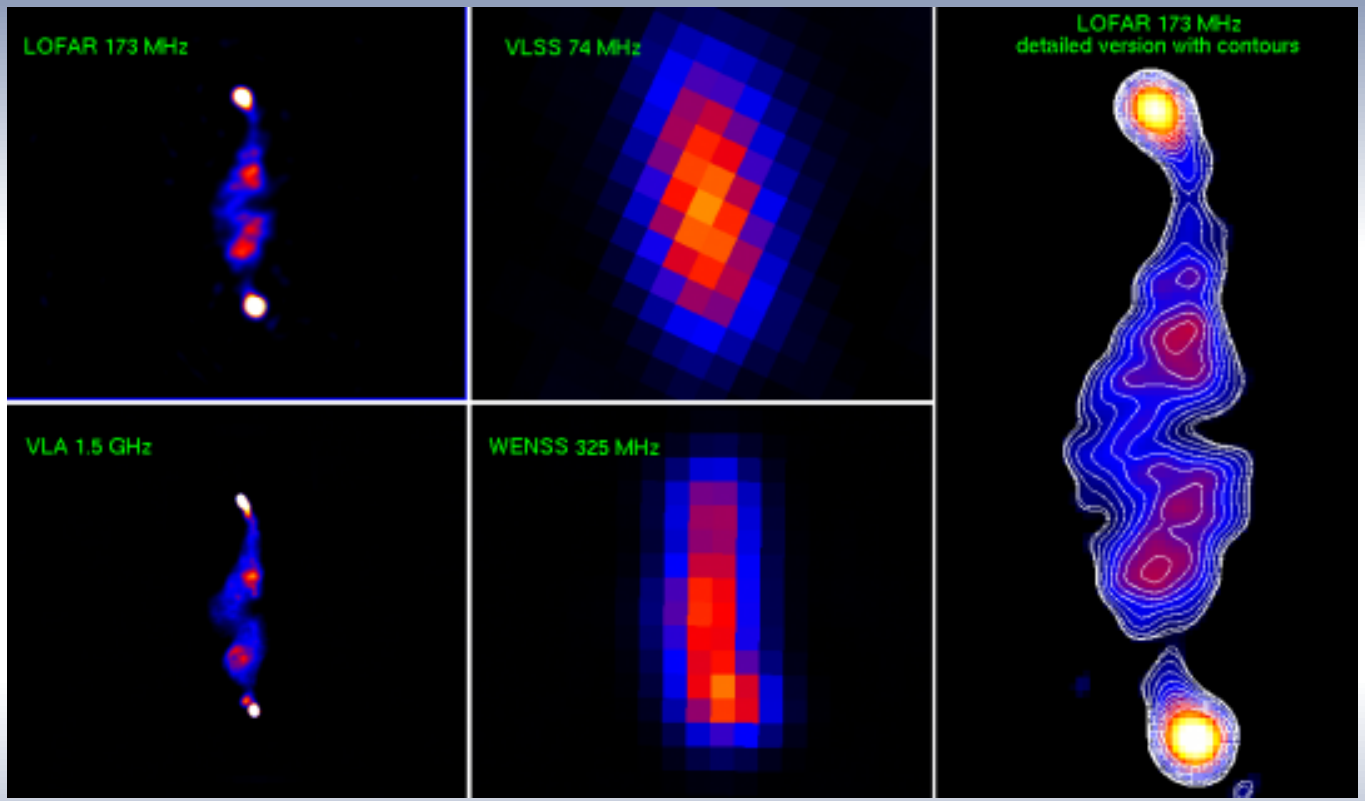

(credit: van Weeren)

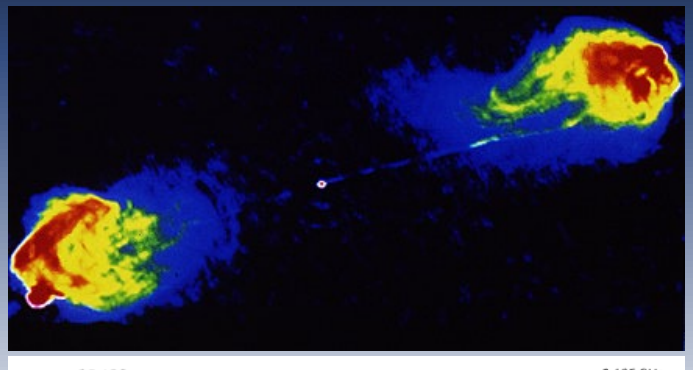

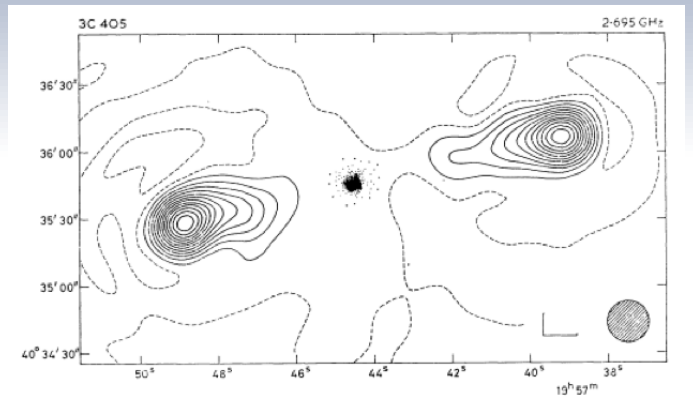

FIG. 1. *The 2·7 GHz contour map. The scale in declination is compressed as indicated by the L shape in the lower right-hand corner, whose arms are each 10″ arc; the shaded disc represents the half power beam width of the instrument. The contour interval corresponds to a brightness temperature of 10 000 °K.*

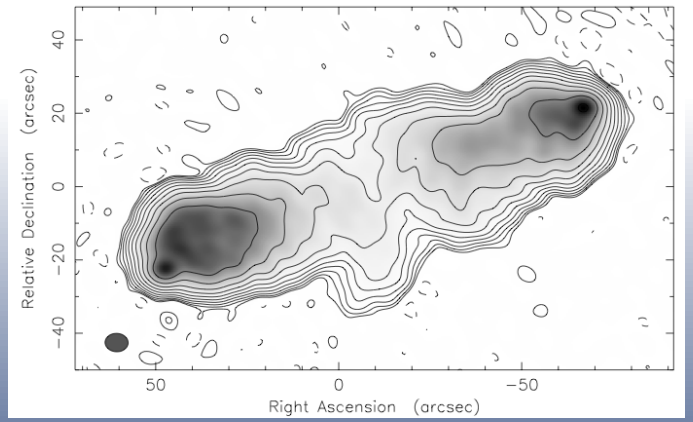

(credit: U.Nijmegen)

Reading List

High Energy Astrophysics, **Longair**, CUP 2011, ISBN: 0-521-75618-1

Physical Processes in the Interstellar Medium, **Spitzer**, Wiley 1998, ISBN: 0-471-29335-0

Tools of Radio Astronomy, **Rohlfs & Wilson**, Springer-Verlag 1996, ISBN: 978-3540609810

Interferometry and Synthesis in Radio Astronomy, **Thompson, Moran & Swenson**, Wiley 2001, ISBN: 0-471-25492-4

Optical and Digital Imaging: Fundamental and Applications, **eds. Cristobal, Schelkens & Thienpont**, Wiley 2011, ISBN: 0-978-3-527-40956-3